Apoptosis (2016) 21:1366–1385
DOI 10.1007/s10495-016-1306-6

The cardioprotective effect of dihydromyricetin prevents ischemia–reperfusion-induced apoptosis in vivo and in vitro via the PI3K/Akt and HIF-1α signaling pathways

Shasha Liu[1] · Qidi Ai[2] · Kai Feng[3] · Yubing Li[4] · Xiang Liu[1]

Published online: 13 October 2016

Abstract Reperfusion therapy is widely used to treat acute myocardial infarction (AMI). However, further injury to the heart induced by rapidly initiating reperfusion is often encountered in clinical practice. A lack of pharmacological strategies in clinics limits the prognosis of patients with myocardial ischemia-reperfusion injury (MIRI). Dihydromyricetin (DMY) is one of the most abundant components in vine tea, commonly known as the tender stems and leaves of *Ampelopsis grossedentata*. The aim of this study was to evaluate the cardioprotection of DMY against myocardial ischemia-reperfusion (I/R) injury and to further investigate the underlying mechanism. An I/R injury was induced by left anterior descending coronary artery occlusion in adult male rats in vivo and a hypoxia–reoxygenation (H/R) injury in H9c2 cardiomyocytes in vitro. We found that DMY pretreatment provided significant protection against I/R-induced injury, including enhanced antioxidant capacity and inhibited apoptosis in vivo and in vitro. This effect correlated with the activation of the PI3K/Akt and HIF-1α signaling pathways. Conversely, blocking Akt activation with the PI3K inhibitor LY294002 effectively suppressed the protective effects of DMY against I/R-induced injury. In addition, the PI3K inhibitor partially blocked the effects of DMY on the upregulation of Bcl-2, Bcl-xl, procaspase-3, -8, and -9 protein expression and the downregulation of HIF-1α, Bnip3, Bax, Cyt-c, cleaved caspase-3, -8, and -9 protein expression. Collectively, these results showed that DMY decreased the apoptosis and necrosis by I/R treatment, and PI3K/Akt and HIF-1α plays a crucial role in protection during this process. These observations indicate that DMY has the potential to exert cardioprotective effects against I/R injury and the results might be important for the clinical efficacy of AMI treatment.

Keywords Dihydromyricetin · Myocardial ischemia–reperfusion · Hypoxia–reoxygenation · Apoptosis · PI3K/Akt · HIF-1α

Abbreviations

DMY	Dihydromyricetin
AMI	Acute myocardial infarction
MIRI	Myocardial ischemia–reperfusion injury
I/R	Ischemia–reperfusion
LAD	Left anterior descending coronary artery
TTC	2,3,5-Triphenyltetrazolium chloride
ECG	Electrocardiogram
HE	Hematoxylin–eosin
H/R	Hypoxia–reoxygenation
MTT	3-(4,5-Dimethyl-2-thiazolyl)-2,5-diphenyl-2-*H*-tetrazolium bromide
DMSO	Dimethyl sulfoxide

Electronic supplementary material The online version of this article (doi:10.1007/s10495-016-1306-6) contains supplementary material, which is available to authorized users.

✉ Xiang Liu
liuxiangtougao@163.com

[1] Pharmacy Department, Xiangtan Central Hospital, No. 120, Heping Road, Yuhu District, Xiangtan 411100, People's Republic of China

[2] School of Pharmaceutical Science, Hunan University of Chinese Medicine, Changsha 410208, People's Republic of China

[3] Oral Surgery, Dalian Stomatological Hospital, Dalian 116021, People's Republic of China

[4] Pharmacy Department, Dalian (Municipal) Friendship Hospital, Dalian 116001, People's Republic of China

LDH	Lactate dehydrogenase
SOD	Superoxide dismutase
MDA	Malondialdehyde
GSH-Px	Glutathione peroxidase
CAT	Catalase from *Micrococcus lysodeikticus*
ROS	Reactive oxygen species
TUNEL	Transferase-mediated deoxyuridine triphosphate-biotin nick end labeling
PI3K	Phosphoinositide 3-kinase
Akt	Protein kinase B
HIF	Hypoxia-inducible factor
Bnip3	Bcl-2/adenovirus E1B 19 kDa protein-interacting protein 3
Cyt-c	Cytochrome C
Bcl-2	B-cell lymphoma-2
Bax	B-cell lymphoma-2-associated x
Bcl-xl	B-cell lymphoma-extra large

Introduction

Acute myocardial infarction (AMI) is the major cause of death and disability worldwide [1, 2]. Current therapies for AMI involve reperfusion of the affected area via thrombolytic therapy or angioplasty. However, ischemia/hypoxia followed by reperfusion induces further death of cardiomyocytes (myocardial ischemia–reperfusion injury [MIRI]), which involves arrhythmia, an expansion of the infarct size and persistent ventricular systolic dysfunction [3, 4]. MIRI is the primary reason for the poor prognosis of AMI [5]. Therefore, novel therapeutic medicine is urgently required to limit the extent of MIRI after AMI.

Currently, the underlying mechanisms of MIRI regulation are still poorly understood. Different mechanisms, including oxidative stress, inflammatory response, apoptosis and metabolism, contribute to MIRI [6]. Oxidative stress is a state of cellular redox imbalance in which the production of reactive oxygen species (ROS) overwhelms the endogenous antioxidant enzyme system. Excessive ROS can damage the myocardial by triggering mitochondrial dysfunction and apoptosis [7]. Apoptosis is a process of programmed cell death that occurs in multicellular organisms, and it is initiated shortly after the onset of myocardial infarction and becomes significantly enhanced during reperfusion [8]. Previous studies have shown that apoptosis serves an important function in AMI and MIRI [9]. Therefore, antioxidant treatment has been proposed to prevent oxidative stress-induced apoptosis. Antioxidant treatment can attenuate MIRI and improve cardiac function and has important clinical significance in AMI.

Ampelopsis grossedentata, a well-known traditional Chinese herbal plant, the tender stems and leaves of which is commonly known as vine tea, are used as a medicinal herb in traditional Chinese medicine. DMY is the primary active ingredient in vine tea. Modern pharmacological research has demonstrated that DMY has many pharmacological activities, including scavenging of free radicals, anti-oxidative, anti-inflammatory, anti-thrombotic, anti-alcoholic, anti-lipid peroxidation, cough relieving, anti-mirobial, anti-hypertensive, hepaprotective, and anti-carcinogenic effects [10–22]. Recent study have demonstrated the potential value of DMY as a rational cardioprotective agent of Adriamycin by protecting the myocardial cells from apoptosis [23].

The phosphoinositide 3-kinase (PI3K)–Akt signaling pathway plays an important role in the control of cardiomyocyte survival and function [24]. Activation of the PI3K/Akt pathway may be useful in promoting myocyte survival in the damaged heart [25]. Hypoxia-inducible factor (HIF) transcription factors plays great role as master regulators of gene expression in response to hypoxia and comprises a set of transcription factors that regulate the expression of approximately 200 genes, which can affect the cellular adaptive responses to hypoxia or ischemia [26, 27]. HIF comprising α and β subunits. HIF-1α-dependent genes such as heme oxygenase-1, inducible nitric oxide synthase, cyclooxygnease-2, and vascular endothelial growth factor can regulate cell survival in ischemia/reperfusion (I/R) [28–31]. HIF-1α also activates the transcription of pro-death genes such as Bcl-2 family members Bcl-2/adenovirus E1B 19-kDa protein-interacting protein 3 (Bnip3). Bnip3 is a BH3-only protein primarily localized in the mitochondria, which is a significant contributor to I/R injury by inducing mitochondrial dysfunction [32, 33]. Therefore, determining whether DMY activates PI3K/Akt and HIF-1α to suppress I/R-induced cardiac injury is of considerable interest.

Most importantly, the present study aims to investigate the potential molecular mechanisms underlying the protective effect of DMY on I/R-induced myocardial injury in rats and H/R-induced cardiotoxicity in H9c2 cardiomyocytes, with a focus on the PI3K/Akt and HIF-1α pathways.

Materials and methods

Materials

Dihydromyricetin (molecular weight = 320.25; purity > 98 %; molecular structure shown in Fig. 1) was purchased from Shanghai Winherb Medical S&T Development (Shanghai, China). Pentobarbital sodium was purchased from Merck (Germany). 2,3,5-triphenyltetrazolium chloride (TTC) was purchased from Sigma (St. Louis, MO). 3-(4,5-Dimethylthiazol-2-yl)-2,5-diphenyltetrazolium bromide (MTT) and 5,5′,6,6′-tetrachloro-1,1′,3,3′-tetraethylbenzimidazolylcarbocyanine iodide (JC-1) were obtained from Enzo Life Sciences (PA, USA). Rat ROS ELISA kit was purchased from

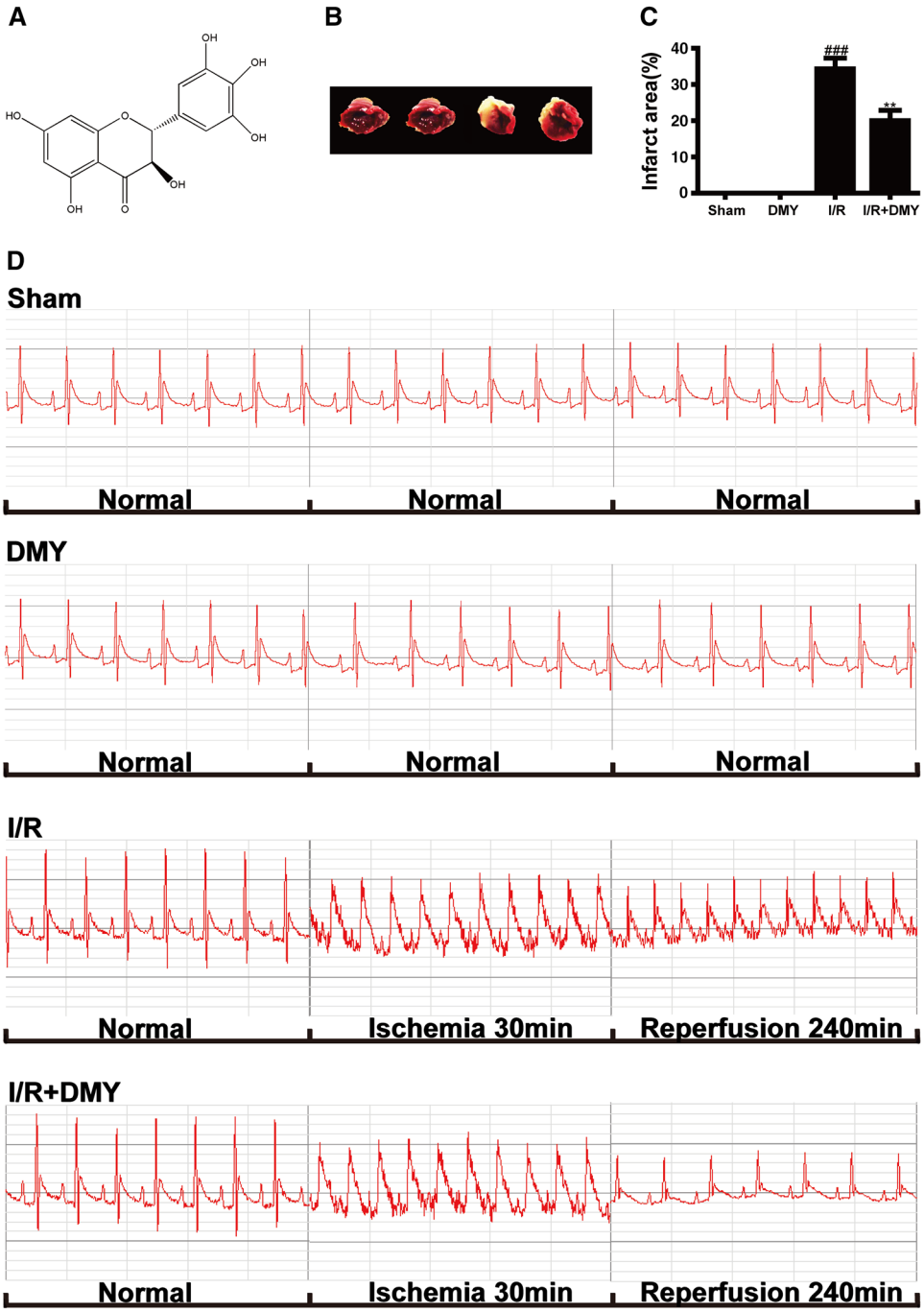

Fig. 1 Molecular structure of dihydromyricetin and dihydromyricetin pretreatment inhibit I/R-induced myocardial injury. **a** Molecular structure of DMY. **b** The myocardial infarct size of each rats assessed by the TTC assay. **c** Quantitative analysis of myocardial infarct size. **d** Effects of DMY treatment on the rat ECG pattern. The results are presented as the mean ± SD from three independent experiments. $^{\#}P < 0.05$ versus sham; $^{\#\#}P < 0.01$ versus sham; $^{\#\#\#}P < 0.001$ versus sham; $^{*}P < 0.05$ versus I/R-treated groups; $^{**}P < 0.01$ versus I/R-treated groups; $^{***}P < 0.001$ versus I/R-treated groups

RapidBio Lab (Calabasas, CA, USA). The Annexin V/Propidium Iodide (PI) assay kit was purchased from Invitrogen (CA, USA). The Caspase-3, -8, and -9 Fluorometric Assay Kit and the Terminal Deoxynucleotidyl Transferase Biotin-dUTP Nick End Labeling (TUNEL) Staining Kit were acquired from BioVision (CA, USA). The Image-iT™ LIVE Green Reactive Oxygen Species Detection Kit and Hoechst 33342 were acquired from Life Technologies (CA, USA). The kits for determining lactate dehydrogenase (LDH), superoxide dismutase (SOD), malondialdehyde (MDA), glutathione peroxidase (GSH-Px), catalase (CAT), and the Coomassie Protein Assay Kit were obtained from the Nanjing Jiancheng Institute of Biological Engineering (Nanjing, China). The Tissue Protein Extraction Kits, Mammalian Protein Extraction Kits, Nuclear and Cytoplasmic Extraction Kit, Protease Inhibitor Cocktail, BCA Protein Assay Kit, and Enhanced Chemiluminescence Western Blot Detection Kits were supplied by CWbiotech (Beijing, China). Specific kinase inhibitor LY294002 (CID: 3973) was purchased from Calbiochem (CA, USA). All of the antibodies were obtained from Santa Cruz Biotechnology (Santa Cruz, CA), and the other chemicals were obtained from Sigma (St. Louis, MO).

Animals and experiment protocols

Male Sprague-Dawley (SD) rats, weighing 250–270 g, were used throughout the experiments. The animals were housed under standard laboratory conditions, (temperature 25 ± 1 °C, humidity 60 %, and light from 6 a.m. to 6 p.m.), given standard rodent chow, and allowed free access to water. All procedures were approved by the Animal Care and Use Committee of China Pharmaceutical University and conform to the revised Guide for the Care and Use of Laboratory Animals published by the US National Institute of Health (NIH) Publication Nos. 85-23 (1996).

A total of 80 SD rats were randomly assigned to four groups: 1, Sham; 2, DMY (150 mg/kg) combined with Sham; 3, I/R treatment; 4, I/R combined with DMY (150 mg/kg). Groups 1 and 3 were administered intragastrically with the saline, groups 2 and 4 were administered intragastrically with DMY (150 mg/kg) for 7 days. In days 8, rats in the groups 3 and 4 were treated with the surgery of ligation the Left anterior descending coronary artery (LAD), whereas the rats in groups 1 and 2 were treated with the same surgical procedures except ligation of the LAD was not performed.

Myocardial ischemia/reperfusion injury procedure

The myocardial I/R model was induced by ligating the LAD for 30 min followed by 4 h of reperfusion. Briefly, adult male SD rats (250–270 g) were anesthetized by administering pentobarbital sodium (40 mg/kg) intraperitoneally. All surgical procedures were carried out under sterile conditions. Following tracheal intubation, the myocardial infarction was produced by performing a left thoracotomy at fourth rib, exposing the heart, placing a 6–0 silk around the LAD, near its origin from the left coronary artery, and making a knot to permanently occlude it. Then, the air was expelled from the chest and the chest was closed. After 30-min of ischemia treatment, reperfusion was allowed for 4 h by releasing the ligation of LAD. The standard electrocardiogram (ECG) limb leads were placed for monitoring ECG changes during the experiments. MIRI was confirmed by an immediate S-T segment elevation of ECG. Sham groups rats were treated with the same surgical procedures except ligation of the LAD was not performed.

Infarct size assessment

The myocardial infarct size was determined by means of a TTC-staining technique and analyzed by a digital imaging system. After 4 h of reperfusion, all the rats were sacrificed, their hearts were excised quickly and placed at −80 °C for 15 min, then sliced into 1-mm-thick sections which incubated for 15 min in 2 % 2,3,5- triphenyltetrazoliumchloride (TTC, Sigma) at 37 °C and photographed with a digital camera. TTC-stained area (red staining, viable tissue), and TTC staining negative area (white, infarct myocardium) were measured digitally with Image Pro Plus software (Media Cybernetics).

Electrocardiography

The standard electrocardiogram (ECG) limb leads were placed for monitoring ECG changes during the experiments. MIRI was confirmed by an immediate S-T segment elevation of ECG. Briefly, rats were anesthetized with pentobarbital sodium (40 mg/kg, i.p.), and electrodes were inserted in the right hind limb, right front limb, and left hind limb. Data were collected using 16-Channel Advanced Research Workstation (MP150, BIOPAC Systems, Inc., CA, USA).

Histo-pathological examination

The apex of the heart was fixed in 4 % paraformaldehyde, routinely processed, and embedded in paraffin. Paraffin Sect. (3 mm) were cut on glass slides, stained with hematoxylin and eosin (HE), and examined under a light microscope (CKX41, Olympus, Tokyo, Japan) by a pathologist blinded to the groups studied.

Measurement of serum enzyme levels in cardiac tissues

After the rats were sacrificed, blood was collected and centrifuged. The levels of LDH activities in the serum was measured according to the manufacturer's instructions (Nanjing Jiancheng Biotechnology Institute, China).

Measurement of antioxidant enzyme activities in cardiac tissues

The antioxidant enzymes, including SOD, MDA, GSH-Px, and CAT activities in heart homogenates were measured according to the manufacturer's instructions (Nanjing Jiancheng Biotechnology Institute, China).

Measurement of ROS activity in cardiac tissues

The ROS activities in heart homogenates was measured by ROS ELISA kit according to the manufacturer's instructions (RapidBio Lab, USA).

Measurement of caspase-3, -8, and -9 activities in cardiac tissues

The Caspase-3, -8, and -9 activities in heart homogenates were measured by Caspase-3, -8, and -9 Fluorometric Assay Kit according to the manufacturer's instructions (BioVision, USA).

TUNEL staining in cardiac tissues

TUNEL was used to detect apoptosis [34]. The deparaffinized and rehydrated heart slices were incubated with proteinase K (20 mg/ml) for 15 min at room temperature. Rinsed with equilibration buffer, the slices were incubated with working-strength terminal deoxynucleotidyl transferase enzyme for 1 h at 37 °C in a humidified chamber. After rinsing in a stop/wash buffer, the sections were incubated with working-strength anti-digoxigenin conjugate at room temperature for 30 min. The slices were stained with 496-diamidino-2-phenylindole and morphological analysis was performed via fluorescence microscopy (Leica, Germany Q9). The results were analyzed using the Image-Pro Plus 6.0 software.

Western blotting analysis of cardiac tissues

After I/R treatment, the whole protein and the cytoplasmic protein of the heart homogenates were obtained using a Tissue and Nuclear and Cytoplasmic Protein Extraction Kit (Cyt-c) with a Protease Inhibitor Cocktail (CWbiotech, Beijing, China). The protein concentration was determined using a BCA Kit (CWbiotech, Beijing, China). Equal amounts of protein were separated by electrophoresis in 10 % sodium dodecyl sulfate polyacrylamide gels and were transferred to nitrocellulose membranes. The membrane was incubated overnight at 4 °C with the following primary antibodies: p-Akt 1/2/3 (B-5): sc-271966; Akt 1/2/3 (H-136): sc-8312; HIF-1α (H-206): sc-10790; Bnip3 (Ana40): sc-56167; Bcl-2 (N-19): sc-492; Bax (N-20): sc-493; Bcl-xl (H-5): sc-8392; Cytochrome-c (A-8): sc-13156; Caspase-3 p11 (C-6): sc-271759; Caspase-8 p18 (D-8): sc-5263; Caspase-9 p10 (H-83): sc-7885; and β-actin (C-2): sc-8432. The membranes were incubated at room temperature with their respective secondary antibodies for 3 h at a room temperature after washing with Tris-buffered saline and Tween 20 (TBST). The blots were developed using Enhanced Chemiluminescence Western Blot Detection Kits (CWbiotech, Beijing, China) after rewashing with TBST and were visualized using molecular imager lab software (BIO-RAD, USA). At least three independent experiments were performed to confirm changes in protein levels.

Cell culture and hypoxia–reoxygenation

Rat embryonic cardiomyoblast-derived H9c2 cardiomyocytes were purchased from the Cell Bank of the Chinese Academy of Sciences (Shanghai, China). All of the cell culture materials were supplied by GIBCO (Grand Island, NY). H9c2 cardiomyocytes were cultured in high-glucose DMEM supplemented with 10 % (v/v) fetal bovine serum and 1 % penicillin/streptomycin (v/v). The cardiomyocytes were maintained at 37 °C with 100 % relative humidity in a CO_2 incubator containing 5 % CO_2. We changed the high-glucose DMEM medium to non-glucose DMEM to mimic ischemia. The H9c2 cardiomyocytes were incubated at 37 °C in an anaerobic glove box (Coy Laboratory, USA) in which the air was removed by a pump and replaced with 5 % H_2 and 95 % N_2. After 6 h of hypoxia, we removed the cells from the anaerobic glove box and replaced the medium with high-glucose medium. The cardiomyocytes were maintained in a regular incubator to mimic reperfusion. The control cardiomyocytes were incubated under normal conditions with high-glucose DMEM.

Cell viability analysis

Cell viability was determined using an MTT assay. H9c2 cardiomyocytes were plated at a density of 1×10^5 cells/ml in 96-well plates and grown for 24 h. First, the cardiomyocytes underwent 6 h of hypoxia treatment; then, cell viability was determined at 0, 3, 6, 9, 12, 18, and 24 h after reoxygenation to determine the optimal molding conditions. Subsequently, 20 μl of 5 mg/ml MTT solution was added to each well, and the cardiomyocytes were incubated for 4 h. The supernatants were aspirated, and the formazan crystals in each well were dissolved in 150 μl of dimethyl sulfoxide (DMSO). Absorbance was measured at 570 nm on a microplate reader (Spectrafluor, TECAN, Sunrise, Austria). The optimal molding conditions were identified; then, the cells were incubated with different concentrations of DMY (12.5, 25, and 50 μM) for 24 h. We evaluated cell viability under normal conditions to determine whether the DMY treatment could lead to cell proliferation and have a cytotoxic effect. The cardiomyocytes were then evaluated under optimal molding conditions to identify the optimal concentration.

Clonogenic assay

In order to determine whether the DMY treatment could lead to cell proliferation and have a cytotoxic effect, H9c2 cardiomyocytes treated with different concentrations of DMY (12.5, 25, and 50 μM) were detached with 5mM EDTA and plated into 6-well tissue culture plates. To allow for colony formation, the plates were incubated for 7 days. The colonies were fixed with 3:1 methanol/acetic acid and stained with 0.1 % crystal violet and 2.1 % citric acid. Colonies containing >50 cells were counted for cell survival.

Cytotoxicity analysis

The following four sets of experiments were performed: (1) control cardiomyocytes; (2) cardiomyocytes pretreated with DMY for 24 h; (3) H/R cardiomyocytes; and (4) H/R cardiomyocytes pretreated with DMY for 24 h. Cell death

was evaluated using the LDH assay. H9c2 cardiomyocytes (3×10^5 cells/well) were fostered in 6-well plates. After treatment, the medium was collected to measure LDH release using LDH assay kits following the manufacturer's instructions.

Determination of the levels of oxidative stress in H9c2 cardiomyocytes

H9c2 cardiomyocytes (3×10^5 cells/well) were seeded into poly-L-lysine-coated 6-well plates for 24 h. After treatment, the cardiomyocytes were harvested to determine the levels of SOD, MDA, GSH-Px and CAT (Nanjing Jiancheng Bioengineering Institute, China). A Coomassie Protein Assay Kit was used to detect the cell protein concentration. A microplate reader was used (Spectrafluor, TECAN, Sunrise, Austria) to obtain the results.

Detection of intracellular ROS production

The effect of DMY on intracellular ROS levels was measured using an Image-iT™ LIVE Green Reactive Oxygen Species Detection Kit according to the manufacturer's instructions (CA, USA). First, we prepared a 10 mM carboxy-H_2DCFDA stock solution and a 25 μM carboxy-H_2DCFDA working solution. After treatment, the cardiomyocytes were harvested, placed into 5 ml round-bottom polystyrene tubes, and washed with phosphate-buffered saline (PBS). Subsequently, the cardiomyocytes were centrifuged for 5 min at 400×*g* at room temperature, and the supernatant was discarded. A sufficient amount of 25 μM carboxy-H_2DCFDA working solution was applied to cover the cardiomyocytes adhering to the coverslip(s). The mixture was incubated (protected from light) for 30 min at 37 °C. The cardiomyocytes were analyzed using a microplate reader (Spectrafluor, TECAN, Sunrise, Austria).

Caspase-3, -8, and -9 activity assay in H9c2 cardiomyocytes

Caspase-3, -8, and -9 activation was measured using a Fluorescein Active Staining Kit (BioVision, CA, USA) according to the manufacturer's instructions. After treatment, nearly 300 μl (1×10^6 cells/ml) of the cardiomyocytes was incubated with 1 μl of substrate FITC-DEVD-FMK for 1 h at 37 °C and then centrifuged at 3000 rpm for 5 min. After removing the supernatant and washing twice with cold PBS, the cardiomyocytes were re-suspended in 100 μl of wash buffer and were maintained to each well in the black microtiter plate on ice. Finally, the samples were analyzed using a microplate reader (Spectrafluor, TECAN, Sunrise, Austria).

Hoechst 33342 and PI double staining

Cardiomyocytes were double-stained with Hoechst 33342 and PI to quantitatively analyze apoptosis. H9c2 cardiomyocytes (1×10^5 cells/well) were grown in 24-well plates for 24 h. After treatment, the cardiomyocytes were then washed twice with PBS and incubated with 10 μg/ml Hoechst 33342 for 15 min at 37 °C in the dark. PI (100 μg/ml) was added (Invitrogen, CA, USA). Stained nuclei were immediately observed using a fluorescence microscope (Leica, Germany Q9). The results were analyzed using the Image-Pro Plus 6.0 software.

Flow cytometric detection of apoptosis

An Annexin V-FITC/PI apoptosis kit was used for flow cytometry to measure the percentage of early apoptosis and necrosis according to the manufacturer's instructions (Invitrogen). After treatment, the cardiomyocytes were harvested, washed twice with cold PBS, and incubated with 5 μl of FITC-Annexin V and 1 μl of PI working solution (100 μg/ml) for 15 min in the dark at room temperature. Cellular fluorescence was measured by flow cytometry analysis with a flow cytometer (FACS Calibur™, BD Biosciences, CA, USA).

TUNEL staining in H9c2 cardiomyocytes

TUNEL was used to detect apoptosis [34]. H9c2 cardiomyocytes (1×10^5 cells/well) were cultured in 24-well plates for 24 h. After treatment, H9c2 cardiomyocytes were fixed by incubation in a 10 % neutral buffered formalin solution at room temperature for 30 min. H9c2 cardiomyocytes were incubated with a methanol solution containing 0.3 % H_2O_2 for 30 min to stop the activity of endogenous peroxidase. Then H9c2 cardiomyocytes were treated with a permeabilizing solution (0.1 % sodium citrate and 0.1 % Triton X-100) at 4 °C for 2 min and were incubated in TUNEL reaction mixture for 60 min at 37 °C. Morphological analysis was performed via fluorescence microscopy (Leica, Germany Q9). Four fields were randomly selected from each sample, and at least 100 cells were counted to calculate the rate of apoptosis. The results were analyzed using the Image-Pro Plus 6.0 software.

Measurement of mitochondrial membrane potential

Changes in mitochondrial membrane potential were detected by JC-1 staining. H9c2 cardiomyocytes (1×10^5 cells/well) were cultured in 24-well plates. After treatment, the cardiomyocytes were harvested and incubated with JC-1 (2 μM final concentration) at 37 °C in the dark for 30 min.

The cardiomyocytes were immediately observed using a fluorescence microscope (Leica, Germany Q9). The results were analyzed with the Image-Pro Plus 6.0 software.

Western blotting analysis of H9c2 cardiomyocytes

H9c2 cardiomyocytes (3×10^5 cells/well) were seeded into poly-L-lysine-coated 6-well plates for 24 h. After treatment, the whole protein and the cytoplasmic protein of the cardiomyocytes were obtained using a Mammalian and Nuclear and Cytoplasmic Protein Extraction Kit (Cyt-c) with a Protease Inhibitor Cocktail (CWbiotech, Beijing, China). The protein concentration was determined using a BCA Kit (CWbiotech, Beijing, China). Western blot analysis was performed in the same manner described above. In the specified experiments, the cells were pretreated with PI3K/Akt inhibitor LY294002 (50 μM) for 1 h, followed by incubation with DMY under H/R conditions. At least three independent experiments were performed to confirm changes in protein levels.

Statistical analyses

All of the data were expressed as the mean ± standard deviation (SD). Data were analyzed using the Student's t-test or one-way ANOVA followed by the Turkey's test or were analyzed using two-way ANOVA followed by Bonferroni's multiple comparison test with Prism 5.00 software. A statistical significance was considered as $P < 0.05$. All of the data were subjected to at least three separate experiments.

Results

Protection against I/R-induced myocardial injury through in vivo dihydromyricetin administration

Dihydromyricetin prevents on I/R-induced myocardial injury

The myocardial infarct size of each rat assessed by the TTC assay is shown in Fig. 1. There was no ischemic damage in the Sham and DMY alone group. Compared with the sham group, myocardial infarct size of I/R group is significantly increased. DMY pronouncedly reduced the myocardial infarct size compared to I/R treatment group. These results showed DMY (150 mg/kg) pretreatment could decrease the myocardial I/R injury (Fig. 1b, c).

ECG patterns of rats are shown in Fig. 1d. Sham and DMY group alone showed normal ECG pattern, whereas I/R treatment group showed remarkable elevation in S-T segment, which indicates the success of myocardial ischemia model. The S-T segment elevation was diminished by pretreatment with DMY (150 mg/kg) in I/R treatment group.

An overall view of the distribution of myocardial damage at the light microscopy level was shown in Fig. 2a. No obvious abnormalities were observed in sham and DMY alone group, while severe myocardial damages were found in I/R treatment group, characterized by myocardial edeam, eosinophilic changeintense, cytoplasmic vacuolization, and contraction band anomaly. Pretreatment with DMY (150 mg/kg) group prevented marked cardiomyocytic vacuolization induced by I/R treatment.

To assay the function of DMY on cardiac injury protection, LDH leakage was measured in different animal groups. As shown in Fig. 2b, I/R induced a greater release of LDH compared with the sham group, and DMY (150 mg/kg) significantly inhibited the release of LDH compared with the I/R treatment group.

Dihydromyricetin enhanced antioxidant capacity in cardiac tissues

I/R induced oxidative stress damage in cardiac tissues, as indicated by decreased SOD, CAT, and GSH-Px activities and increased lipid peroxidation (MDA production); however, these changes were effectively alleviated by DMY (Fig. 2c–f).

ROS generation is among the common responses to cell damage and contributes to the progression of apoptosis [35]. As shown in Fig. 2g, the I/R-induced group exhibited increased ROS levels compared with the sham group, and the DMY (150 mg/kg) pretreatment significantly attenuated I/R-induced ROS release in cardiac tissues. Therefore, ROS generation was involved in the protection provided by DMY against I/R-induced myocardial injury.

Dihydromyricetin treatment inhibited I/R-induced apoptosis in cardiac tissues

The activation of caspase-3 was explored to confirm the characteristic features of apoptosis in I/R-treated cardiac tissues. The activation of caspase-3 is one of the key processes involved in apoptosis and contributes to myocardial dysfunction [36]. Compared to I/R-treated group, myocardial caspase-3 activation was reduced in DMY-pretreated group (Fig. 2h). Apoptotic damage was also activated in the I/R-treated cardiac tissues (Fig. 2i, j), as shown by elevated caspase-8 and caspase-9 activities. DMY (150 mg/kg) pretreatment ameliorated the apoptotic damage compared with the I/R treatment group.

DNA fragmentation is the characteristic feature of cells undergoing apoptosis. TUNEL were used to detect these features. I/R treatment remarkably increased the the number of TUNEL-positive cells (Fig. 3a). The TUNEL-positive cell rate increased significantly compared to the sham group (Fig. 3c), which suggested that I/R induces phosphatidylserine

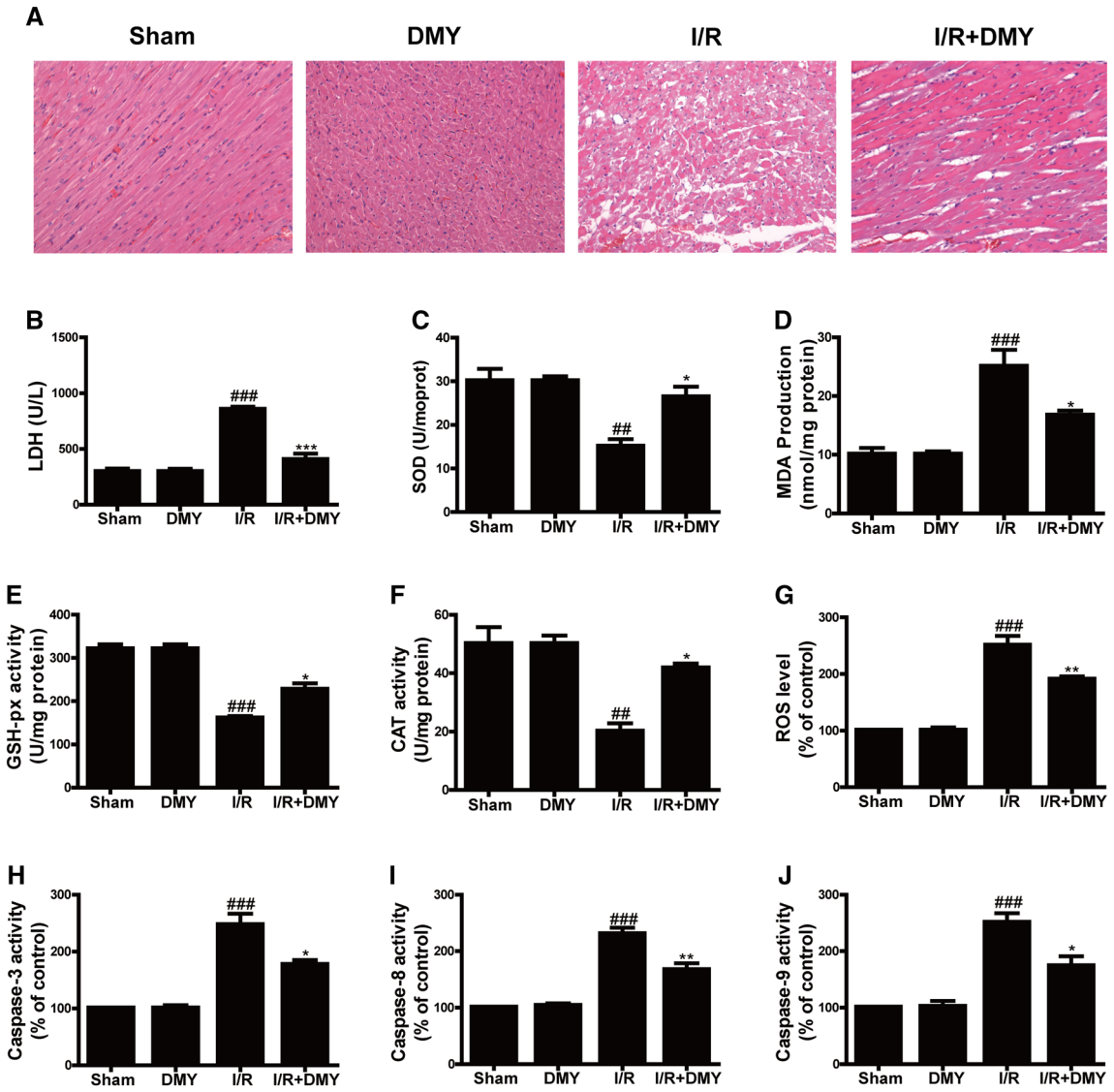

Fig. 2 Dihydromyricetin pretreatment inhibit I/R-induced myocardial injury and the antioxidant and anti-apoptotic capacity of dihydromyricetin. **a** Effects of DMY on histological changes in rat hearts by HE staining. **b** Effects of DMY on LDH level in cardiac tissues was measured using an LDH assay kit. **c** Effects of DMY on the activity of SOD in cardiac tissues. **d** Effects of DMY on the activity of MDA in cardiac tissues. **e** Effects of DMY on the activity of GSH-Px in cardiac tissues. **f** Effects of DMY on the activity of CAT in cardiac tissues. **g** ROS levels were measured using a fluorometric assay. **h** DMY attenuation of I/R-induced caspase-3 activity, as evaluated by fluorometric assay. **i** DMY attenuation of I/R-induced caspase-8 activity, as evaluated by fluorometric assay. **j** DMY attenuation of I/R-induced caspase-9 activity, as evaluated by fluorometric assay. $^{\#}P<0.05$ versus sham; $^{\#\#}P<0.01$ versus sham; $^{\#\#\#}P<0.001$ versus sham; $^{*}P<0.05$ versus I/R-treated groups; $^{**}P<0.01$ versus I/R-treated groups; $^{***}P<0.001$ versus I/R-treated groups

externalization and DNA fragmentation in cardiac tissues. DMY (150 mg/kg) pretreatment effectively ameliorated the I/R-induced DNA fragmentation (Fig. 3c).

Exploring the protection mechanism by Western blotting analysis in cardiac tissues

To explore the signaling pathways that could contribute to the anti-apoptotic effect of DMY, the kinetics of DMY mediated Akt and HIF-1α activation were examined. As shown in Fig. 3, the DMY-mediated increase in p-Akt expression, which was decreased by I/R injury (Fig. 3d). DMY also mediated decrease in HIF-1α and Bnip3 expression, which was increased by I/R injury (Fig. 3e, f). Therefore, the PI3K/Akt and HIF-1α signaling pathways are involved in the anti-apoptotic effect of DMY.

To elucidate the protective mechanism of DMY, we examined the levels of apoptotic proteins in cardiac tissues. The results showed that DMY (150 mg/kg) could inhibit I/R-induced apoptosis (Fig. 4a). The Bcl-2 family, including Bcl-2, Bax, and Bcl-xl, plays an important role in

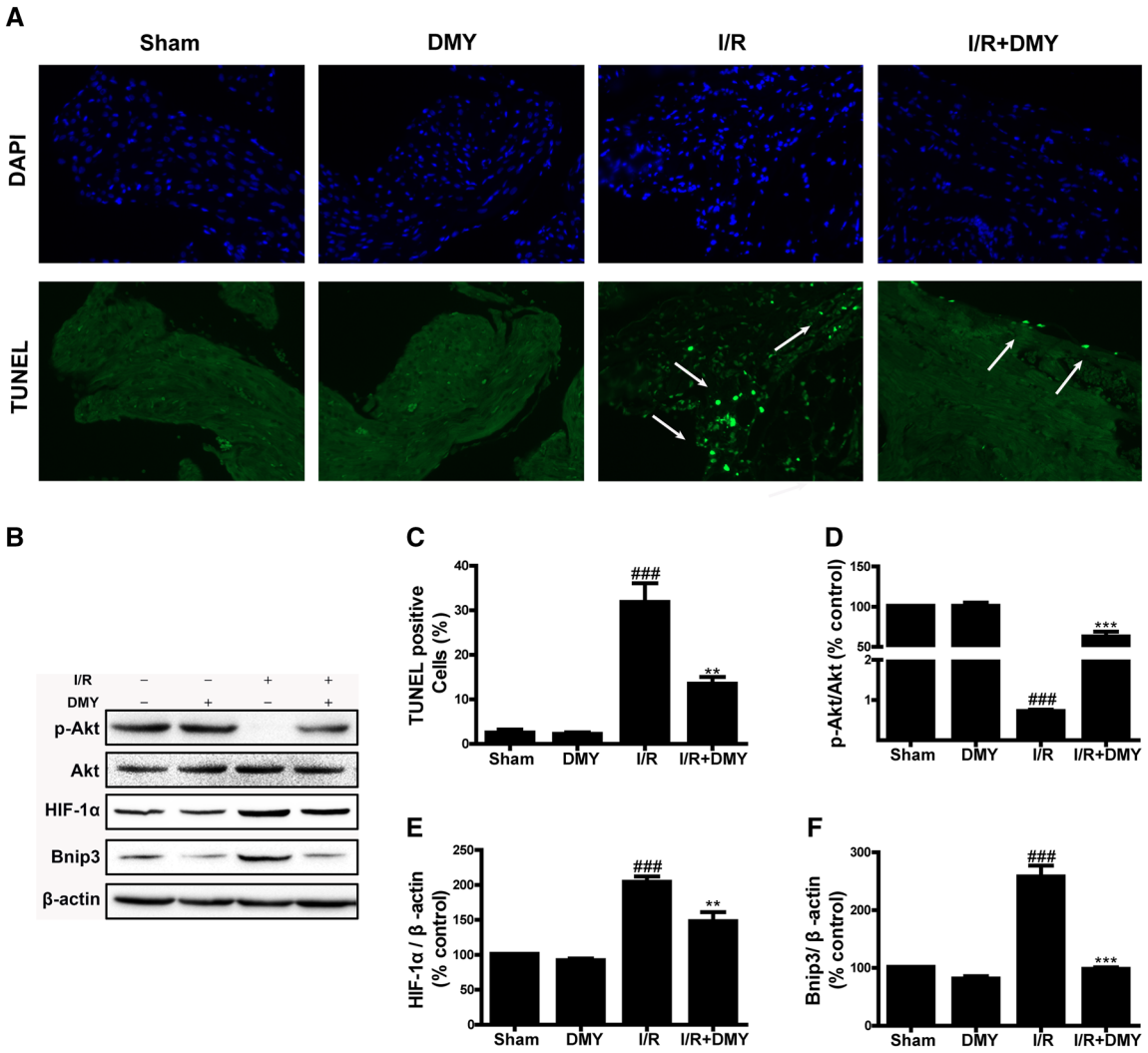

Fig. 3 Dihydromyricetin attenuates I/R-induced DNA fragmentation and effects of dihydromyricetin on PI3K/Akt and HIF-1α signaling pathways. **a** Fluorescence microscopy images of TUNEL staining. **b** Effects of I/R and DMY on PI3K/Akt and HIF-1α signaling pathways. **c** Quantitative analysis of TUNEL-positive cell rate. **d** The p-Akt expression in cardiac tissues was assayed by western blotting using a Gel-Pro analyzer. **e** The HIF-1α expression in cardiac tissues was assayed by western blotting using a Gel-Pro analyzer. **f** The Bnip3 expression in cardiac tissues was assayed by western blotting using a Gel-Pro analyzer. $^{\#}P<0.05$ versus sham; $^{\#\#}P<0.01$ versus sham; $^{\#\#\#}P<0.001$ versus sham; $^{*}P<0.05$ versus I/R-treated groups; $^{**}P<0.01$ versus I/R-treated groups; $^{***}P<0.001$ versus I/R-treated groups

H/R-induced apoptosis in various cells [37]. DMY pretreatment can increase the Bcl-2/Bax ratio and the level of Bcl-xl expression (Fig. 4a), which are decreased by H/R damage (Fig. 4b, c). The caspase family also plays an important role in H/R-induced apoptosis in various cells [38]. Procaspase-3, -8, and -9 expression levels decreased after I/R damage, and cleaved caspase-3, -8, and -9 expression levels increased after I/R damage; however, DMY pretreatment could reverse these effects (Fig. 4e–j). Cytochrome-c (Cyt-c) release is the important index of apoptosis [39]. I/R induced the release of Cyt-c, whereas DMY pretreatment inhibited such release. These combined results demonstrate that DMY inhibited I/R-induced apoptosis by upregulating Bcl-2, Bcl-xl, and procaspase-3, -8, and -9 protein expression levels and by downregulating Bax, Cyt-c and cleaved caspase-3, -8, and -9 protein expression levels.

Protective effect of dihydromyricetin against H/R-induced injury in vitro

Effect of H/R on cell viability and dihydromyricetin treatment inhibition of H/R-induced cell death in H9c2 cardiomyocytes

To determine whether DMY could protect against cardiac injury induced by H/R in vitro, we first investigated the reoxygenation conditions leading to cell toxicity in H9c2 cardiomyocytes. After 6 h of hypoxia followed by reoxygenation

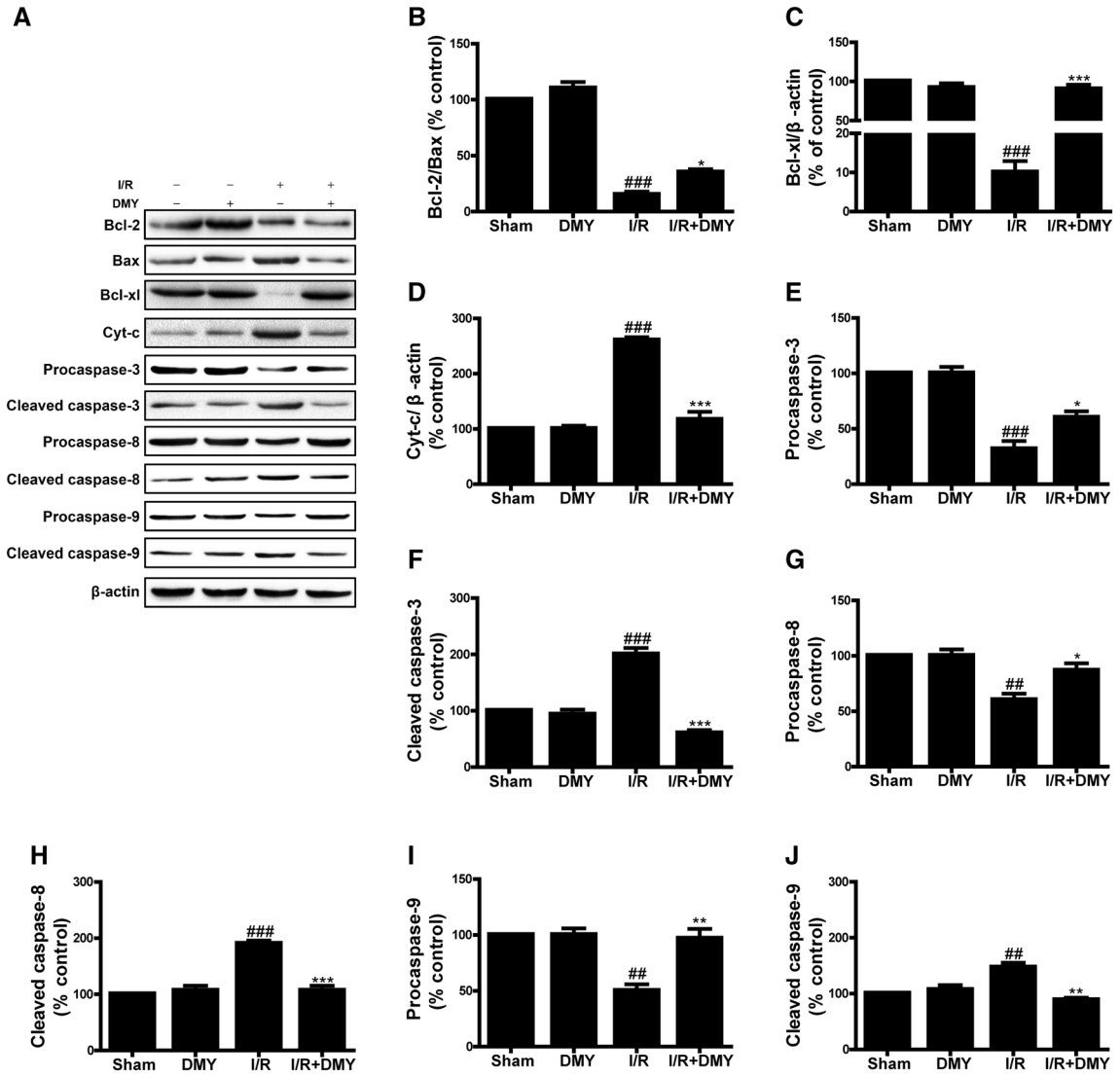

Fig. 4 Effects of dihydromyricetin on apoptotic proteins. **a** Effects of I/R and DMY on the Bcl-2 family and the caspase protein family. **b** The Bcl-2/Bax expression ratio in cardiac tissues was assayed by western blotting using a Gel-Pro analyzer. **c** The Bcl-xl expression in cardiac tissues was assayed by western blotting analysis using a Gel-Pro analyzer. **d** The Cyt-c expression in cardiac tissues was assayed by western blotting analysis using a Gel-Pro analyzer. **e** The procaspase-3 expression in cardiac tissues was assayed by western blotting analysis using a Gel-Pro analyzer. **f** The cleaved caspase-3 expression in cardiac tissues was assayed by western blotting analysis using a Gel-Pro analyzer. **g** The procaspase-8 expression in cardiac tissues was assayed by western blotting analysis using a Gel-Pro analyzer. **h** The cleaved caspase-8 expression in cardiac tissues was assayed by western blotting analysis using a Gel-Pro analyzer. **i** The procaspase-9 expression in cardiac tissues was assayed by western blotting analysis using a Gel-Pro analyzer. **j** The cleaved caspase-9 expression in cardiac tissues was assayed by western blotting analysis using a Gel-Pro analyzer. $^{\#}P<0.05$ versus sham; $^{\#\#}P<0.01$ versus sham; $^{\#\#\#}P<0.001$ versus sham; $^{*}P<0.05$ versus I/R-treated groups; $^{**}P<0.01$ versus I/R-treated groups; $^{***}P<0.001$ versus I/R-treated groups

treatment, cell viability was examined at 0, 3, 6, 9, 12, 18, and 24 h after reoxygenation using an MTT assay. The cardiomyocytes in the control group were considered to be 100 % viable. As shown in Fig. 5a, 6 h of hypoxia reduced cell viability by approximately 14.67 %, and reoxygenation led to a further time-dependent decline in cell viability. The viability of cardiomyocytes was reduced by approximately 31.86 % at 24 h after reoxygenation.

To identify the optimal dosage of DMY to protect against H/R-induced H9c2 cardiomyocyte injury, we evaluated the possibility that DMY may have a proliferation or a cytotoxic effect on H9c2 cardiomyocytes.

After 24 h of treatment with various DMY concentrations (12.5, 25, and 50 μM), no change in cell viability was detected by the MTT assay in H9c2 cardiomyocytes (Fig. 5b). In order to confirm these results, clonogenic assay

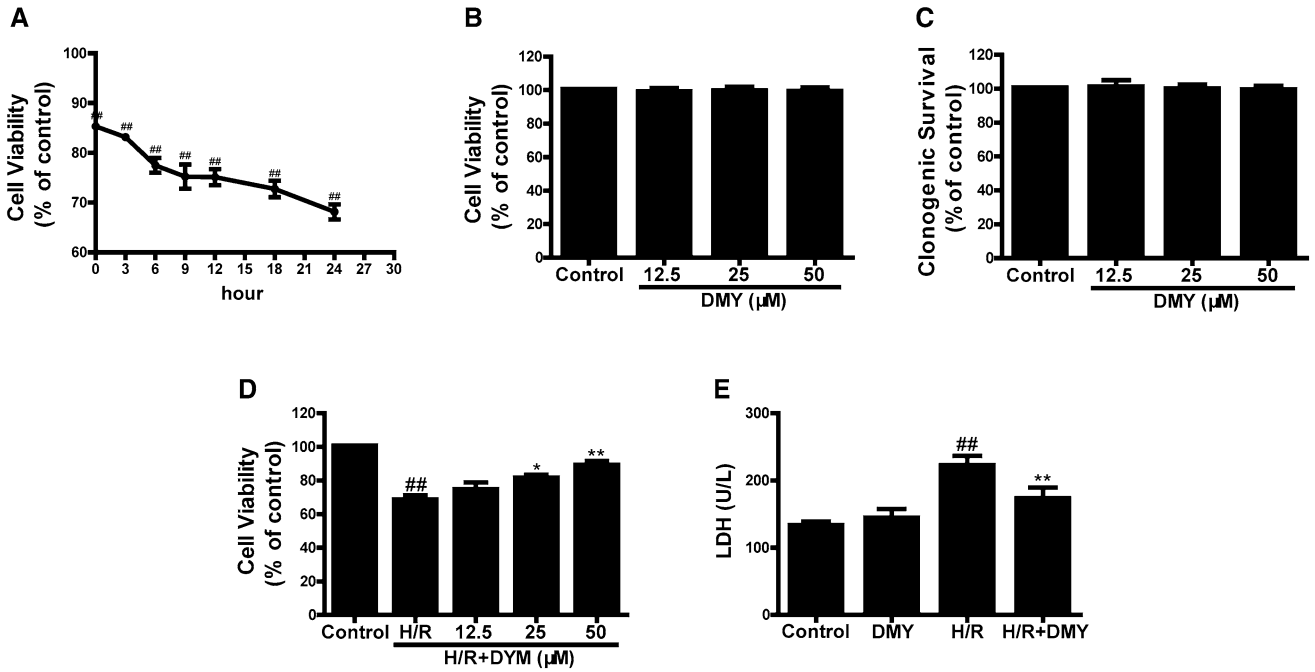

Fig. 5 Effects of H/R on cell viability and dihydromyricetin pretreatment inhibit H/R-induced cell death in H9c2 cardiomyocytes. **a** Effects of H/R on H9c2 cardiomyocytes. H9c2 cardiomyocytes were exposed to hypoxia for 6 h followed by reoxygenation for 24 h. Cell viability was examined at 0, 3, 6, 9, 12, 18, and 24 h after reoxygenation using an MTT assay. **b** Cell viability was not significantly affected by DMY (12.5, 25, and 50 μM) based on the results of the MTT assay. **c** Cell clonogenic survival was not significantly affected by DMY (12.5, 25, and 50 μM) based on the results of the clonogenic assay. **d** H9c2 cardiomyocytes were pretreated with DMY (12.5, 25, and 50 μM) for 24 h before H/R treatment. Cell viability was determined by an MTT assay. **e** Effects of DMY on LDH level in H9c2 cardiomyocytes was measured using an LDH assay kit. The results are presented as the mean ± SD from three independent experiments. $^{\#}P < 0.05$ versus control; $^{\#\#}P < 0.01$ versus control; $^{\#\#\#}P < 0.001$ versus control; $^{*}P < 0.05$ versus H/R-treated cells; $^{**}P < 0.01$ versus H/R-treated cells; $^{***}P < 0.001$ versus H/R-treated cells

was used. After 24 h of treatment with various DMY concentrations (12.5, 25, and 50 μM) and incubated for 7 days, no change in cell viability was detected by the clonogenic assay in H9c2 cardiomyocytes (Fig. 5c). Thus, our results excluded the possibility that DMY treatment changes cellular viability.

After excluding the possibility of changes in proliferation and cytotoxicity, we determined the best DMY dosage for protection against H/R-induced damage to H9c2 cardiomyocytes. We treated H9c2 cardiomyocytes with various DMY concentrations (12.5, 25, and 50 μM) for 24 h. The cardiomyocytes were exposed to 6 h of hypoxia followed by 24 h of reoxygenation. We identified the optimal dosage as 50 μM (Fig. 5d).

LDH leakage is an indicator of cell death and was examined. As shown in Fig. 5e, the following four sets of conditions were examined: (1) control cells; (2) cells pretreated with DMY (50 μM) for 24 h; (3) H/R cells; and (4) H/R cells pretreated with DMY (50 μM) for 24 h. H/R induced a greater release of LDH compared with the control group, and DMY significantly inhibited the release of LDH compared with the H/R group.

Dihydromyricetin enhanced antioxidant capacity in H9c2 cardiomyocytes

H/R induced oxidative stress damage in H9c2 cardiomyocytes, as indicated by decreased SOD, CAT, and GSH-Px activities and increased lipid peroxidation (MDA production); however, these changes were effectively alleviated by DMY (Fig. 6a–d).

ROS generation is among the common responses to cell damage and contributes to the progression of apoptosis [35]. As shown in Fig. 6e, the H/R-induced group exhibited increased intracellular ROS levels compared with the control group, and the DMY pretreatment significantly attenuated H/R-induced ROS release in H9c2 cardiomyocytes. Therefore, ROS generation was involved in the protection provided by DMY against H/R-induced cell injury.

Dihydromyricetin treatment inhibited H/R-induced cell apoptosis in H9c2 cardiomyocytes

Apoptotic cell death was examined to investigate the type of cell death in H9c2 cardiomyocytes exposed to H/R and to

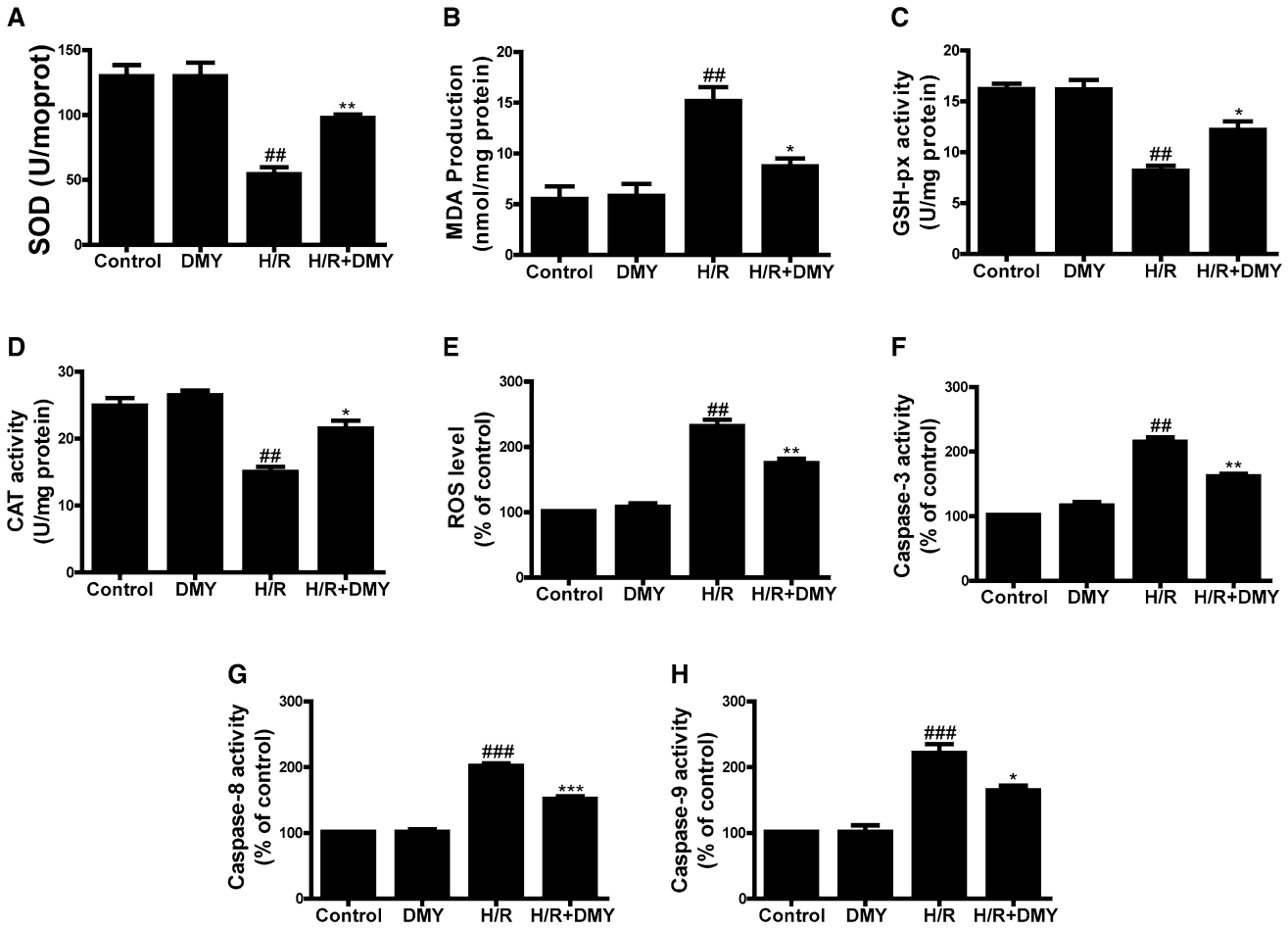

Fig. 6 The antioxidant and anti-apoptotic capacity of dihydromyricetin. H9c2 cardiomyocytes were exposed to hypoxia for 6 h followed by reoxygenation for 24 h. **a** Effects of DMY on the activity of SOD in H9c2 cardiomyocytes. **b** Effects of DMY on the activity of MDA in H9c2 cardiomyocytes. **c** Effects of DMY on the activity of GSH-Px in H9c2 cardiomyocytes. **d** Effects of DMY on the activity of CAT in H9c2 cardiomyocytes. **e** The intracellular ROS levels were measured using a fluorometric assay. **f** DMY attenuation of H/R-induced caspase-3 activity, as evaluated by fluorometric assay. **g** DMY attenuation of H/R-induced caspase-8 activity, as evaluated by fluorometric assay. **h** DMY attenuation of H/R-induced caspase-9 activity, as evaluated by fluorometric assay. The results are presented as the mean ± SD from three independent experiments. $^{\#}P < 0.05$ versus control; $^{\#\#}P < 0.01$ versus control; $^{\#\#\#}P < 0.001$ versus control; $^{*}P < 0.05$ versus H/R-treated cells; $^{**}P < 0.01$ versus H/R-treated cells; $^{***}P < 0.001$ versus H/R-treated cells

gain insight into the mechanism underlying the myocardial protection of DMY.

The activation of caspase-3 was explored to confirm the characteristic features of apoptosis in H/R-treated H9c2 cardiomyocytes. The activation of caspase-3 is one of the key processes involved in apoptosis and contributes to myocardial dysfunction [36]. Compared to H/R-treated H9c2 cardiomyocytes, myocardial caspase-3 activation was reduced in DMY-pretreated cardiomyocytes (Fig. 6f). Apoptotic damage was also activated in the H/R-treated H9c2 cardiomyocytes (Fig. 6g, h), as shown by elevated caspase-8 and caspase-9 activities. DMY pretreatment ameliorated the apoptotic damage compared with the H/R treated group.

The morphological changes in apoptotic H9c2 cardiomyocytes induced by H/R were observed using Hoechst 33342/PI staining. Cardiomyocytes with blue nuclei were considered as normal, whereas those with bright blue or red/pink nuclei were considered apoptotic. As shown in Fig. 7a, few cardiomyocytes with bright blue or red/pink nuclear staining were observed in the control group. H9c2 cardiomyocytes treated with H/R clearly exhibited PI staining, which indicates apoptosis. Pretreatment with DMY significantly alleviated the morphological changes triggered by H/R, as shown in Fig. 7c.

Phosphatidylserine externalization and DNA fragmentation are characteristic features of cells undergoing apoptosis. Annexin V/PI double staining and TUNEL were used to detect these features. H/R treatment remarkably increased the proportion of Annexin V/PI-labeled cells (Fig. 7b) and the number of TUNEL-positive cells (Fig. 8a). The TUNEL-positive cell rate increased significantly compared to the control group (Fig. 8c), which suggested that H/R induces phosphatidylserine externalization

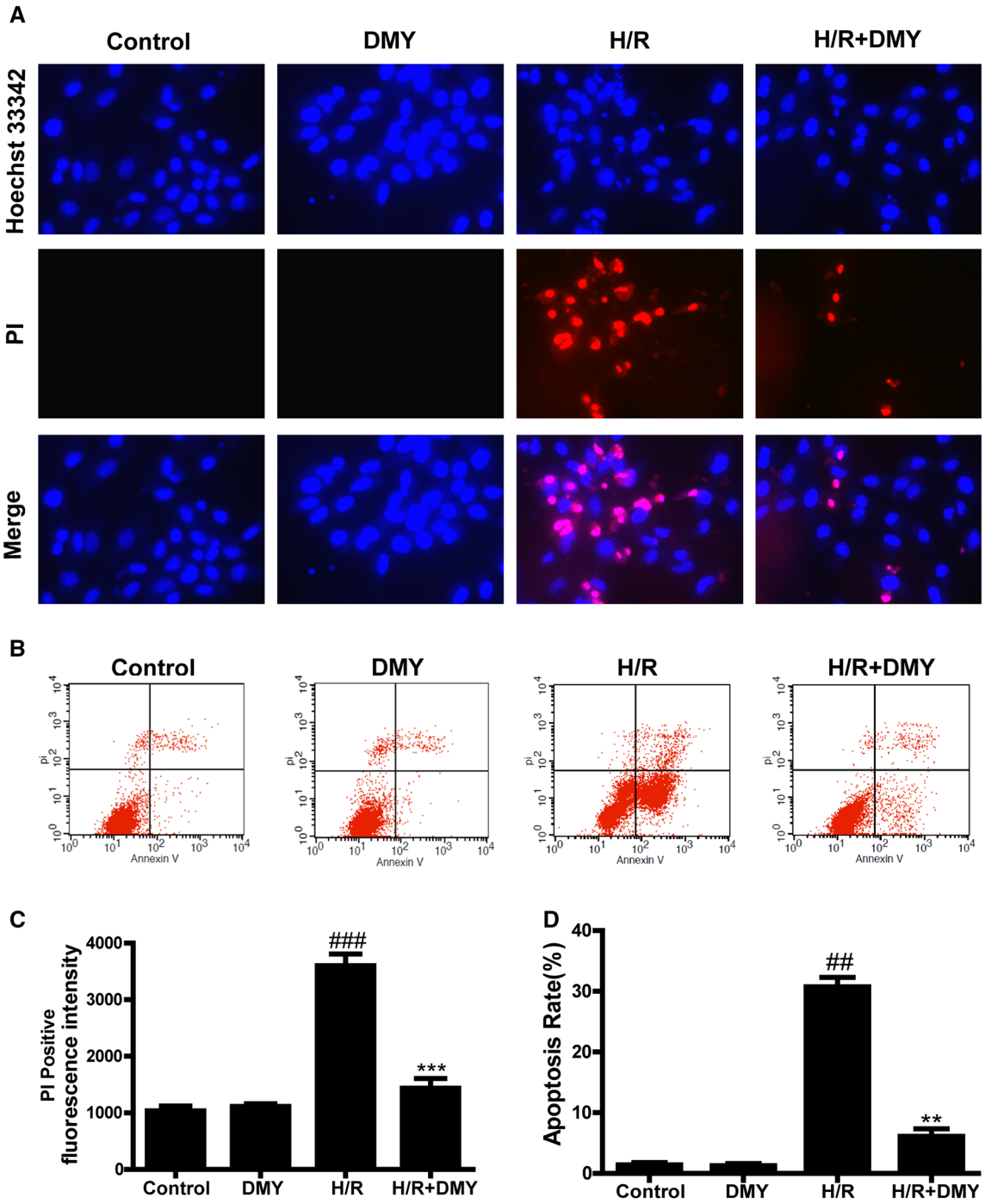

Fig. 7 Effects of H/R on cell apoptosis and dihydromyricetin pretreatment inhibit H/R-induced apoptosis in H9c2 cardiomyocytes. H9c2 cardiomyocytes were exposed to hypoxia for 6 h followed by reoxygenation for 24 h. **a** Cell apoptosis and necrosis were assessed using Hoechst 33342/PI double staining by using fluorescence microscopy. **b** A scatter diagram of apoptotic H9c2 cardiomyocytes detected by Annexin V/PI double staining. **c** Quantitative analysis of PI-positive fluorescence intensity. **d** Quantitative analysis of apoptosis rate, as detected by Annexin V/PI double staining. The results are presented as the mean ± SD from three independent experiments. $^{\#}P < 0.05$ versus control; $^{\#\#}P < 0.01$ versus control; $^{\#\#\#}P < 0.001$ versus control; $^{*}P < 0.05$ versus H/R-treated cells; $^{**}P < 0.01$ versus H/R-treated cells; $^{***}P < 0.001$ versus H/R-treated cells

and DNA fragmentation in H9c2 cardiomyocytes. DMY pretreatment effectively reduced the proportion of cardiomyocytes that were apoptotic (Fig. 7d) and ameliorated the H/R-induced DNA fragmentation (Fig. 8c).

We also explored the intrinsic mitochondrial apoptotic pathway using the depolarization of the mitochondrial membrane to confirm the characteristics of apoptosis in H/R-treated H9c2 cardiomyocytes. A significant increase

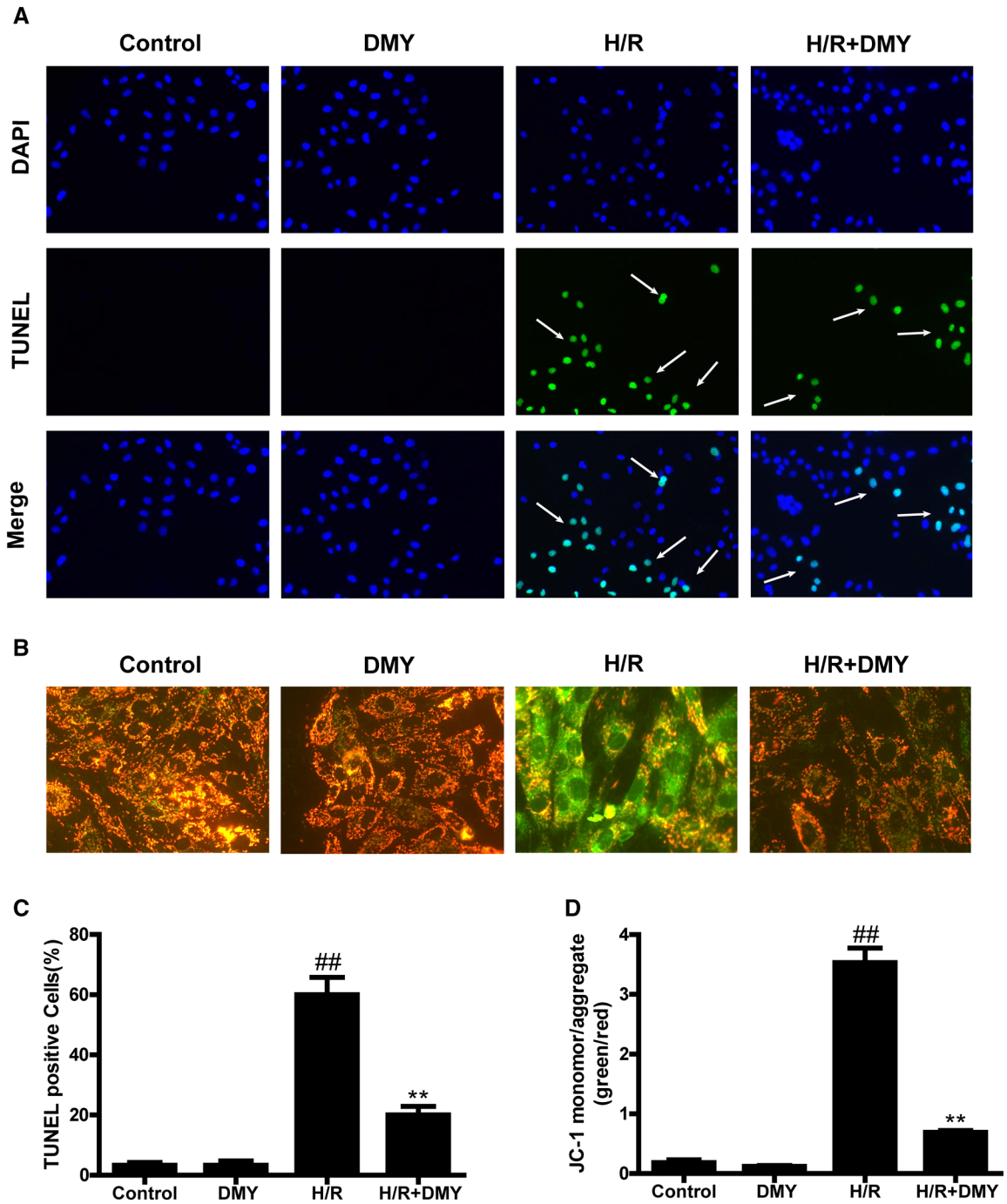

Fig. 8 Dihydromyricetin attenuates H/R-induced DNA fragmentation and mitochondrial apoptotic cell death. H9c2 cardiomyocytes were exposed to hypoxia for 6 h followed by reoxygenation for 24 h. **a** Fluorescence microscopy images of TUNEL staining. **b** Fluorescence microscopy images of JC-1 staining. **c** Quantitative analysis of TUNEL-positive cell rate. **d** Quantitative analysis of the JC-1 monomer/aggregate rate. The results are presented as the mean ± SD from three independent experiments. $^{\#}P < 0.05$ versus control; $^{\#\#}P < 0.01$ versus control; $^{\#\#\#}P < 0.001$ versus control; $^{*}P < 0.05$ versus H/R-treated cells; $^{**}P < 0.01$ versus H/R-treated cells; $^{***}P < 0.001$ versus H/R-treated cells

was observed in the percentage of cells that displayed a decreased mitochondrial membrane potential after H/R treatment (Fig. 8b). This finding suggested that H/R depolarized the mitochondrial membrane of H9c2 cardiomyocytes. DMY pretreatment could increase the mitochondrial membrane potential (Fig. 8d).

Exploring the protection mechanism by Western blotting analysis in H9c2 cardiomyocytes

To explore the signaling pathways that could contribute to the anti-apoptotic effect of DMY, the kinetics of DMY mediated Akt and HIF-1α activation were examined. To determine whether DMY-induced Akt activation is responsible for its cell protective effect, the effect of blocking the PI3K-Akt pathway on DMY-induced cell protection was determined using the PI3K/Akt inhibitor LY294002. As shown in Fig. 9, the DMY-mediated increase in p-Akt expression, which was decreased by H/R injury, was blocked by LY294002. DMY-mediated decrease in HIF-1α and Bnip3 expression, which was increased by H/R injury, was also blocked by LY294002 (Fig. 9). Therefore, the PI3K/Akt and HIF-1α signaling pathways are involved in the anti-apoptotic effect of DMY and HIF-1α is the downstream regulator of PI3K/Akt.

To elucidate the protective mechanism of DMY, we examined the levels of apoptotic proteins in H9c2 cardiomyocytes; LY294002 was also used. The results showed that DMY could inhibit H/R-induced apoptosis (Fig. 10a). DMY pretreatment can increase the Bcl-2/Bax ratio and the level of Bcl-xl expression (Fig. 10a), which are decreased by H/R damage (Fig. 10b, c), whereas the effects were completely reversed by LY294002 (Fig. 10b, c). Procaspase-3, -8, and -9 expression levels decreased after H/R damage, and cleaved caspase-3, -8, and -9 expression levels increased after H/R damage; however, DMY pretreatment could reverse these effects (Fig. 10e–j). The DMY-mediated increase in procaspase-3, -8, and -9 expression and the

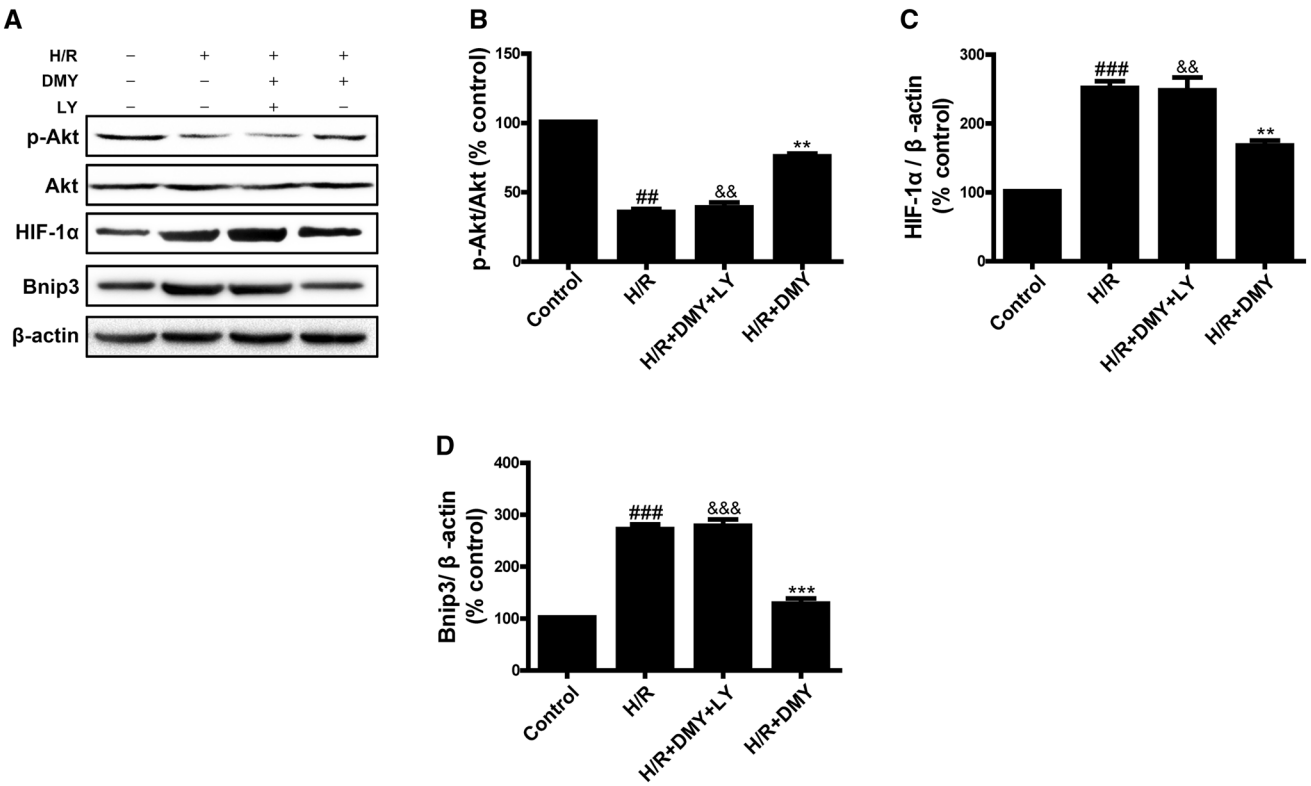

Fig. 9 Specific kinase inhibitor was used to confirm the effects of dihydromyricetin on PI3K/Akt and HIF-1α signaling pathways. H9c2 cardiomyocytes were exposed to hypoxia for 6 h followed by reoxygenation for 24 h. **a** Effects of H/R and DMY on PI3K/Akt and HIF-1α signaling pathways. **b** The p-Akt expression in H9c2 cardiomyocytes was assayed by western blotting using a Gel-Pro analyzer. **c** The HIF-1α expression in cardiac tissues was assayed by western blotting using a Gel-Pro analyzer. **d** The Bnip3 expression in cardiac tissues was assayed by western blotting using a Gel-Pro analyzer. The results are presented as the mean ± SD from three independent experiments. $^{\#}P < 0.05$ versus control; $^{\#\#}P < 0.01$ versus control; $^{\#\#\#}P < 0.001$ versus control; $^{\&}P < 0.05$ versus H/R-treated cells pretreated with DMY; $^{\&\&}P < 0.01$ versus H/R-treated cells pretreated with DMY; $^{\&\&\&}P < 0.01$ versus H/R-treated cells pretreated with DMY; $^{*}P < 0.05$ versus H/R-treated cells; $^{**}P < 0.01$ versus H/R-treated cells; $^{***}P < 0.01$ versus H/R-treated cells

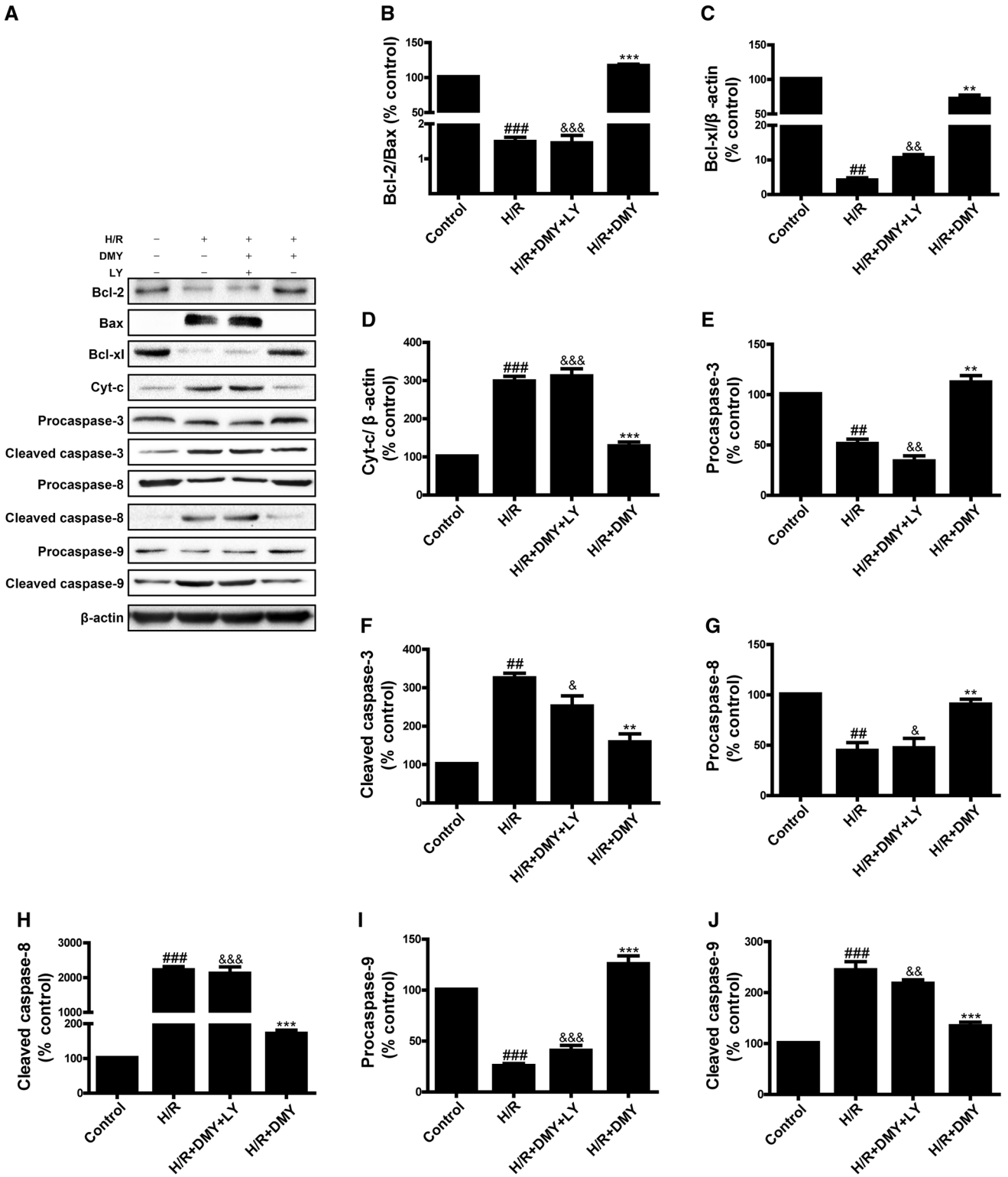

decrease in cleaved caspase-3, -8, and -9 expression were eliminated by LY294002 (Fig. 10e–j). The DMY mediated decrease in Cyt-c expression, which was increased by H/R, was also blocked by LY294002 (Fig. 10d). These combined results further demonstrate that DMY inhibited H/R-induced apoptosis by upregulating Bcl-2, Bcl-xl, and procaspase-3, -8, and -9 protein expression levels and by downregulating Bax, Cyt-c and cleaved caspase-3, -8, and -9 protein expression levels in a PI3K/Akt-dependent manner.

◂**Fig. 10** Specific kinase inhibitor was used to confirm the effects of dihydromyricetin on apoptotic proteins. H9c2 cardiomyocytes were exposed to hypoxia for 6 h followed by reoxygenation for 24 h. **a** Effects of H/R and DMY on the Bcl-2 family and the caspase protein family. **b** The Bcl-2/Bax expression ratio was assayed by western blotting using a Gel-Pro analyzer. **c** The Bcl-xl expression in H9c2 cardiomyocytes was assayed by western blotting analysis using a Gel-Pro analyzer. **d** The Cyt-c expression in H9c2 cardiomyocytes was assayed by western blotting analysis using a Gel-Pro analyzer. **e** The procaspase-3 expression in H9c2 cardiomyocytes was assayed by western blotting analysis using a Gel-Pro analyzer. **f** The cleaved caspase-3 expression in H9c2 cardiomyocytes was assayed by western blotting analysis using a Gel-Pro analyzer. **g** The procaspase-8 expression in H9c2 cardiomyocytes was assayed by western blotting analysis using a Gel-Pro analyzer. **h** The cleaved caspase-8 expression in H9c2 cardiomyocytes was assayed by western blotting analysis using a Gel-Pro analyzer. **i** The procaspase-9 expression in H9c2 cardiomyocytes was assayed by western blotting analysis using a Gel-Pro analyzer. **j** The cleaved caspase-9 expression in H9c2 cardiomyocytes was assayed by western blotting analysis using a Gel-Pro analyzer. The results are presented as the mean ± SD from three independent experiments. $^{\#}P<0.05$ versus control; $^{\#\#}P<0.01$ versus control; $^{\#\#\#}P<0.001$ versus control; $^{\&}P<0.05$ versus H/R-treated cells pretreated with DMY; $^{\&\&}P<0.01$ versus H/R-treated cells pretreated with DMY; $^{\&\&\&}P<0.01$ versus H/R-treated cells pretreated with DMY; $^{*}P<0.05$ versus H/R-treated cells; $^{**}P<0.01$ versus H/R-treated cells; $^{***}P<0.01$ versus H/R-treated cells

Discussion

AMI remains a leading cause of death worldwide, despite recent advancements in pharmacologic and early revascularization therapies. A major factor affecting the prevalence of AMI is MIRI. Compared to reperfusion, reoxygenation causes further cardiomyocyte damage followed by hypoxia-induced changes [40]. Evidence has shown that apoptosis may be responsible for AMI and MIRI. Moreover, apoptosis is always an important research direction for therapeutic applications in AMI [41]. Normal ROS can be scavenged by endogenous antioxidants, which are abundant in tissues [42]. Endogenous ROS can also be scavenged by protective enzymes. Thus, the modulation of ROS and apoptosis levels may represent a novel target for therapeutic interventions.

The principal finding of this study indicated that DMY prevents I/R-induced apoptosis in vivo and in vitro via PI3K/Akt and HIF-1α pathways. This study was the first to demonstrate the cardioprotective effects of DMY against I/R-induced oxidative stress and apoptosis in vivo and in vitro. DMY, the most abundant and bioactive flavonoid extracted from *Ampelopsis grossedentata* (Fig. 1a), exhibits a wide range of pharmacological effects, including antioxidant and anti-apoptotic properties [23, 43]. H/R-induced oxidative damage to H9c2 cardiomyocytes is widely used to mimic oxidative stress [44]. In the present study, I/R-induced apoptosis in vivo and in vitro caused significant increases in LDH release, DNA fragmentation, and apoptosis rates, as well as a marked reduction in cell viability (Figs. 1, 2, 3, 5, 6, 7, 8). The TTC, ECG, and histopathological examination results showed that pretreatment with DMY attenuated myocardial infarct size, improved left ventricular dysfunction, and pathological disorders compare with the I/R group in vivo (Figs. 1, 2). The MTT results of the H/R model showed a time-dependent decrease in cell viability from 0 to 24 h of reoxygenation (Fig. 5a). This result indicated that cell viability decreased in H9c2 cardiomyocytes in response to hypoxia, as further evidenced by their response to reoxygenation. Finally, we selected hypoxia for 6 h and reoxygenation for 24 h as our model in vitro. This model was used to explore the cardioprotective effects of DMY. After observing the proliferation and cytotoxic effects of DMY, we found that preconditioning with DMY at a concentration of 50 μM for 24 h significantly enhanced the survival of H9c2 cardiomyocytes after H/R treatment (Fig. 5b–d). The protective effect of DMY pretreatment is manifested in an increase in cell viability in vitro and a decrease in LDH leakage both in vivo and in vitro (Figs. 2b, 5e). DMY preconditioning could effectively increase the activities of SOD, GSH-Px, and CAT in vivo and in vitro (Figs. 2c, e, f, 6a, c, d). An excessive amount of ROS damages various biomolecules via lipid peroxidation, protein oxidation, and DNA damage, resulting in mitochondrial dysfunction, caspase-3 activation, and cell apoptosis [45]. In the present study, I/R-induced damage increased the ROS concentration in vivo and in vitro (Figs. 2g, 6e), thus increasing the levels of oxidative stress markers, such as lipid peroxidation products (MDA) and DMY pretreatment could decreased these (Figs. 2d, 6b). DMY pretreatment inhibited cellular apoptosis, as evidenced by the decrease in the caspase-3, -8, and -9 level (Figs. 2h–j, 6f–h), the decreasing apoptosis rates in Hoechst 33342/PI double staining (Fig. 7a, c), Annexin V-FITC/PI detection (Fig. 7b, d), and in TUNEL-positive cells in vivo and in vitro (Figs. 3a, c, 8a, c). I/R treatment also caused a remarkable loss of mitochondrial membrane potential in vitro (Fig. 8b, d). However, DMY preconditioning effectively reversed the damage induced by I/R in vivo and in vitro, suggesting that DMY promotes the resistance to I/R-induced oxidative stress. These results suggest that DMY inhibited I/R-induced apoptosis in vivo and in vitro through an anti-oxidation effect. However, the mechanism underlying these cardioprotective effects of DMY remains unclear.

The activation of the Akt-related signaling pathway has been shown to be involved in the regulation of cardiomyocyte apoptosis [46, 47]. A previous study demonstrated that the activation of PI3K and its downstream Akt molecules could suppress cardiomyocyte apoptosis and promote cell survival in ischemic heart [48, 49]. Some studies also demonstrated that HIF-1α involved in the regulation of cardiomyocyte apoptosis [50]. The Western blot results showed that the DMY-mediated increase in p-Akt expression, which was decreased by I/R injury in vivo and in vitro. DMY also

mediated decrease in HIF-1α and Bnip3 expression, which was increased by I/R injury in vivo and in vitro (Figs. 3b, d–f, 9). To elucidate the protective mechanism of DMY, we examined the levels of apoptotic proteins in vivo and in vitro. The results showed that DMY could inhibit I/R-induced apoptosis in vivo and in vitro (Figs. 4a, 9a). DMY inhibited I/R-induced apoptosis by upregulating Bcl-2, Bcl-xl, and procaspase-3, -8, and -9 protein expression levels and by downregulating Bax, Cyt-c and cleaved caspase-3, -8, and -9 protein expression levels (Figs. 4, 9).

Consistent with the protective mechanism of DMY reported previously, our study demonstrated that the addition of the PI3K specific inhibitor LY294002 effectively suppresses the DMY-induced Akt and HIF-1α activation and simultaneously reverses the cell protective effect of DMY in vitro (Fig. 9). This strongly suggests that the protective effect of DMY on H/R-induced cardiomyocyte apoptosis is at least partially mediated by the PI3K/Akt signaling pathway and HIF-1α is the downstream regulator of PI3K/Akt.

The activation of the PI3K/Akt pathway by modulating the activation and expression of Bcl-2 family proteins is essential for cell survival. The Western blot results showed that DMY pretreatment could inhibit H/R-induced apoptosis in H9c2 cardiomyocytes; however, this effect can be reversed by LY294002 treatment (Fig. 9). DMY pretreatment could increase the Bcl-2/Bax ratio, Bcl-xl, and procaspase-3, -8, and -9 expression level, which were decreased by H/R damage (Fig. 9b, c, e, g, i). DMY pretreatment could also decrease the Cyt-c and cleaved caspase-3, -8, and -9 expression levels, which were increased by H/R damage (Fig. 9d, f, h, j). All of the above effects can be reversed by LY294002 treatment (Fig. 9). We propose that the PI3K/Akt and HIF-1α pathways plays a survival role by regulating apoptosis proteins during DMY treatment and protects against I/R-induced apoptosis in vivo and in vitro.

In summary, DMY protects rats and H9c2 cardiomyocytes from I/R-induced injury, as indicated by the morphological changes, LDH activity, oxidative and apoptotic parameters. The protective effect of DMY against I/R-induced apoptosis is dependent on the PI3K/Akt and HIF-1α signaling pathways, and the activation of PI3K/Akt and HIF-1α signaling pathways further modulates changes in the expression and activation of the Bcl-2 family proteins and the caspase family proteins, such as Bcl-2, Bax, Bcl-xl, and caspase-3, -8, and -9, which result in a decreased expression of caspase-3 activity. These data indicate that DMY might attenuate MIRI and improve cardiac function and has important

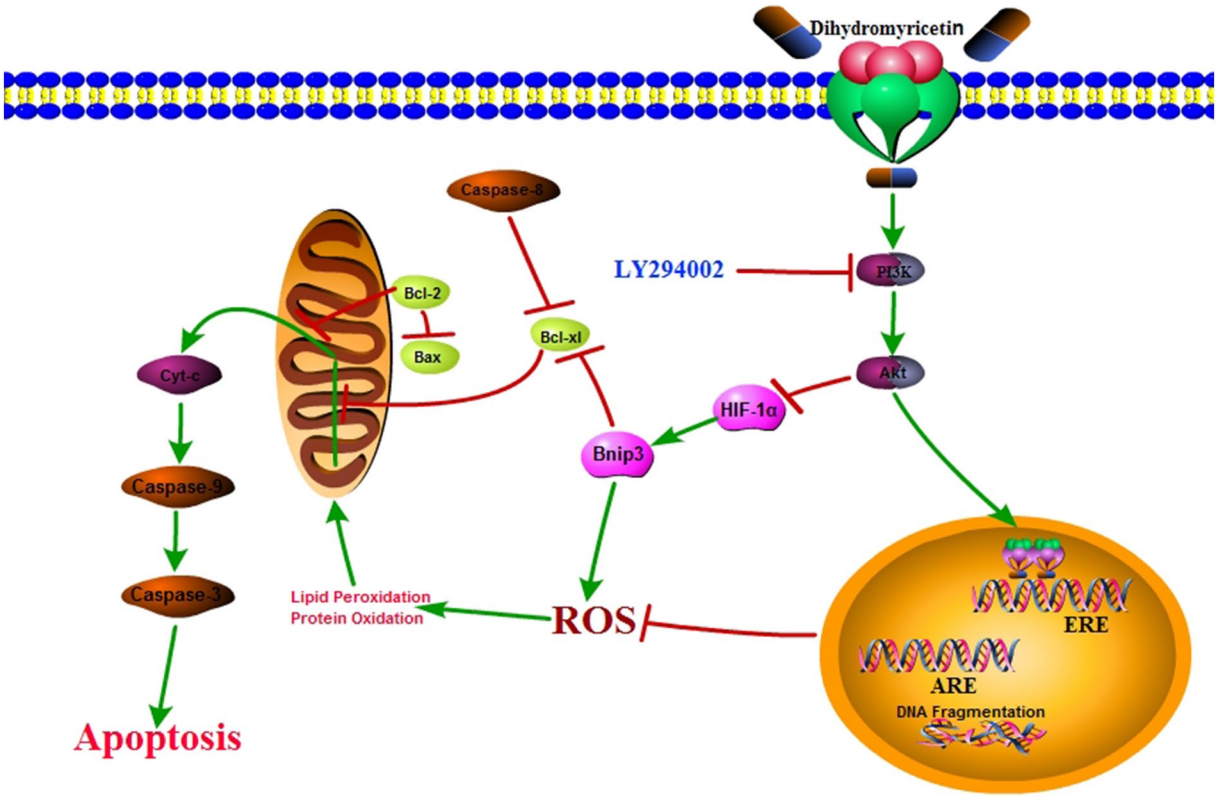

Fig. 11 Schematic of the molecular mechanism responsible for the cardioprotective effects of dihydromyricetin. DMY can prevent H/R-induced apoptosis of H9c2 cardiomyocytes via PI3K/Akt and HIF-1α pathways

clinical significance in AMI. However, this study is still has its limitation. The protective effect of DMY should be confirmed in other apoptosis-related disease models to expand the clinically applied range of DMY. The pharmacokinetic features of DMY in animals and humans should also be considered.

Conclusion

DMY has cardioprotective effects against I/R-induced oxidative stress and apoptosis in vivo and in vitro. A novel mechanism of PI3K/Akt and HIF-1α signaling activation were responsible for the cardioprotective effect of DMY (Fig. 11). This finding may provide novel insights into the mechanism through which DMY mediate PI3K/Akt and HIF-1α signaling activation and the cardioprotective effects of *Ampelopsis grossedentata*.

References

1. Damiani G, Salvatori E, Silvestrini G et al (2015) Influence of socioeconomic factors on hospital readmissions for heart failure and acute myocardial infarction in patients 65 years and older: evidence from a systematic review. Clin Interv Aging 10:237–245
2. Crea F, Battipaglia I, Andreotti F (2015) Sex differences in mechanisms, presentation and management of ischaemic heart disease. Atherosclerosis 241:157–168
3. Hausenloy DJ, Yellon DM (2013) Myocardial ischemia-reperfusion injury: a neglected therapeutic target. J Clin Invest 123:92–100
4. Ai Q, Sun G, Luo Y et al (2015) Ginsenoside Rb1 prevents hypoxia-reoxygenation-induced apoptosis in H9c2 cardiomyocytes via an estrogen receptor-dependent crosstalk among the Akt, JNK, and ERK 1/2 pathways using a label-free quantitative proteomics analysis. RSC Adv 5:26346–26363
5. Hausenloy DJ, Yellon DM (2015) Targeting myocardial reperfusion injury—the search continues. N Engl J Med 373:1073–1075
6. Morrison A, Li J (2011) PPAR-gamma and AMPK-advantageous targets for myocardial ischemia/reperfusion therapy. Biochem Pharmacol 82:195–200
7. Meng X, Sun G, Ye J, Xu H, Wang H, Sun X (2014) Notoginsenoside R1-mediated neuroprotection involves estrogen receptor-dependent crosstalk between Akt and ERK1/2 pathways: a novel mechanism of Nrf2/ARE signaling activation. Free Radic Res 48:445–460
8. Gu J, Fan Y, Liu X et al (2014) SENP1 protects against myocardial ischaemia/reperfusion injury via a HIF1alpha-dependent pathway. Cardiovasc Res 104:83–92
9. Sun Y, Yi W, Yuan Y et al (2013) C1q/tumor necrosis factor-related protein-9, a novel adipocyte-derived cytokine, attenuates adverse remodeling in the ischemic mouse heart via protein kinase A activation. Circulation 128:S113–S120
10. Jiang B, Le L, Pan H, Hu K, Xu L, Xiao P (2014) Dihydromyricetin ameliorates the oxidative stress response induced by methylglyoxal via the AMPK/GLUT4 signaling pathway in PC12 cells. Brain Res Bull 109:117–126
11. Liao W, Ning Z, Ma L et al (2014) Recrystallization of dihydromyricetin from Ampelopsis grossedentata and its anti-oxidant activity evaluation. Rejuvenation Res 17:422–429
12. Shi L, Zhang T, Liang X et al (2015) Dihydromyricetin improves skeletal muscle insulin resistance by inducing autophagy via the AMPK signaling pathway. Mol Cell Endocrinol 409:92–102
13. Chen S, Zhao X, Wan J et al (2015) Dihydromyricetin improves glucose and lipid metabolism and exerts anti-inflammatory effects in nonalcoholic fatty liver disease: arandomized controlled trial. Pharmacol Res 99:74–81
14. Hou XL, Tong Q, Wang WQ et al (2015) Suppression of inflammatory responses by dihydromyricetin, a flavonoid from *Ampelopsis grossedentata*, via inhibiting the activation of NF-kappaB and MAPK signaling pathways. J Nat Prod 78:1689–1696
15. Shen Y, Lindemeyer AK, Gonzalez C et al (2012) Dihydromyricetin as a novel anti-alcohol intoxication medication. J Neurosci 32:390–401
16. Liu P, Zou D, Chen K et al (2015) Dihydromyricetin improves hypobaric hypoxia-induced memory impairment via modulation of SIRT3 signaling. Mol Neurobiol. doi:10.1007/s12035-015-9627-y
17. Guo WZ, Miao YL, An LN et al (2013) Midazolam provides cytoprotective effect during corticosterone-induced damages in rat astrocytes by stimulating steroidogenesis. Neurosci Lett 547:53–58
18. Wang JT, Jiao P, Zhou Y, Liu Q (2016) Protective effect of dihydromyricetin against lipopolysaccharide-induced acute kidney injury in a rat model. Med Sci Monit 22:454–459
19. Liao SF, Wang HT, Yan FX, Zheng YX, Zeng ZW, Zheng WH. (2014) Protective effect and mechanisms of dihydromyricetin on PC12 cells induced by oxidative injury. Zhong yao cai = Zhongyaocai = J Chin Med Mater 37:1014–1020.
20. Xie J, Liu J, Chen TM et al (2015) Dihydromyricetin alleviates carbon tetrachloride-induced acute liver injury via JNK-dependent mechanism in mice. World J Gastroenterol 21:5473–5481
21. Jin MY, Ding Y, Zhang T, Cai ZZ, Tao JS (2014) Simultaneous determination of dihydromyricetin and resveratrol in ampelopsis sinica (Miq.) W.T. Wang by high-performance liquid chromatography coupled with a diode array detection method. J Chromatogr Sci 52:339–343
22. Wong IL, Wang BC, Yuan J et al (2015) Potent and nontoxic chemosensitizer of P-glycoprotein-mediated multidrug resistance in cancer: synthesis and evaluation of methylated epigallocatechin, gallocatechin, and dihydromyricetin derivatives. J Med Chem 58:4529–4549
23. Zhu H, Luo P, Fu Y et al (2015) Dihydromyricetin prevents cardiotoxicity and enhances anticancer activity induced by adriamycin. Oncotarget 6:3254–3267
24. Wang ZG, Wang Y, Huang Y et al (2015) bFGF regulates autophagy and ubiquitinated protein accumulation induced by myocardial ischemia/reperfusion via the activation of the PI3K/Akt/mTOR pathway. Sci Rep 5:9287
25. Han CK, Kuo WW, Shen CY et al (2014) Dilong prevents the high-KCl cardioplegic solution administration-induced apoptosis in H9c2 cardiomyoblast cells mediated by MEK. Am J Chin Med 42:1507–1519
26. Fang Y, Zhang H, Zhong Y, Ding X (2016) Prolyl hydroxylase 2 (PHD2) inhibition protects human renal epithelial cells and mice kidney from hypoxia injury. Oncotarget
27. Jin Y, Zhao X, Zhang H, Li Q, Lu G, Zhao X (2016) Modulatory effect of silymarin on pulmonary vascular dysfunction through HIF-1alpha-iNOS following rat lung ischemia-reperfusion injury. Exp Ther Med 12:1135–1140
28. Wang P, Liang X, Lu Y, Zhao X, Liang J (2016) MicroRNA-93 downregulation ameliorates cerebral ischemic injury through the Nrf2/HO-1 defense pathway. Neurochem Res. doi:10.1007/s11064-016-1975-0
29. Zhu T, Yao Q, Wang W, Yao H, Chao J (2016) iNOS induces vascular endothelial cell migration and apoptosis via autophagy in ischemia/reperfusion injury. Cell Physiol Biochem 38:1575–1588

30. Rayner BS, Duong TT, Myers SJ, Witting PK (2006) Protective effect of a synthetic anti-oxidant on neuronal cell apoptosis resulting from experimental hypoxia re-oxygenation injury. J Neurochem 97:211–221
31. Jiang Y, Li L, Ma J et al (2016) Auricular vagus nerve stimulation promotes functional recovery and enhances the post-ischemic angiogenic response in an ischemia/reperfusion rat model. Neurochem Int 97:73–82
32. Kubli DA, Quinsay MN, Huang C, Lee Y, Gustafsson AB (2008) Bnip3 functions as a mitochondrial sensor of oxidative stress during myocardial ischemia and reperfusion. Am J Physiol Heart Circ Physiol 295:H2025–H2031
33. Kubli DA, Ycaza JE, Gustafsson AB (2007) Bnip3 mediates mitochondrial dysfunction and cell death through Bax and Bak. Biochem J 405:407–415
34. Zhang S, Qi Y, Xu Y et al (2013) Protective effect of flavonoid-rich extract from Rosa laevigata Michx on cerebral ischemia-reperfusion injury through suppression of apoptosis and inflammation. Neurochem Int 63:522–532
35. Sinha K, Das J, Pal PB, Sil PC (2013) Oxidative stress: the mitochondria-dependent and mitochondria-independent pathways of apoptosis. Arch Toxicol 87:1157–1180
36. Li XQ, Cao W, Li T et al (2009) Amlodipine inhibits TNF-alpha production and attenuates cardiac dysfunction induced by lipopolysaccharide involving PI3K/Akt pathway. Int Immunopharmacol 9:1032–1041
37. Peng X, Shao J, Shen Y et al (2013) FAT10 protects cardiac myocytes against apoptosis. J Mol Cell Cardiol 59:1–10
38. Yang ZB, Tan B, Li TB et al (2014) Protective effect of vitexin compound B-1 against hypoxia/reoxygenation-induced injury in differentiated PC12 cells via NADPH oxidase inhibition. Naunyn-Schmiedeberg's Arch Pharmacol 387:861–871
39. Sun J, Li YZ, Ding YH et al (2014) Neuroprotective effects of gallic acid against hypoxia/reoxygenation-induced mitochondrial dysfunctions in vitro and cerebral ischemia/reperfusion injury in vivo. Brain Res 1589:126–139
40. Moens AL, Claeys MJ, Timmermans JP, Vrints CJ (2005) Myocardial ischemia/reperfusion-injury, a clinical view on a complex pathophysiological process. Int J Cardiol 100:179–190
41. Wang Y, Zhang H, Chai F, Liu X, Berk M (2014) The effects of escitalopram on myocardial apoptosis and the expression of Bax and Bcl-2 during myocardial ischemia/reperfusion in a model of rats with depression. BMC Psychiatry 14:349
42. Chen XL, Kunsch C (2004) Induction of cytoprotective genes through Nrf2/antioxidant response element pathway: a new therapeutic approach for the treatment of inflammatory diseases. Curr Pharm Des 10:879–891
43. Meng G, Yang S, Chen Y, Yao W, Zhu H, Zhang W (2015) Attenuating effects of dihydromyricetin on angiotensin II-induced rat cardiomyocyte hypertrophy related to antioxidative activity in a NO-dependent manner. Pharm Biol 53:904–912
44. Sun L, Zang WJ, Wang H et al (2014) Acetylcholine promotes ROS detoxification against hypoxia/reoxygenation-induced oxidative stress through FoxO3a/PGC-1alpha dependent superoxide dismutase. Cell Physiol Biochem 34:1614–1625
45. Radak Z, Zhao Z, Goto S, Koltai E (2011) Age-associated neurodegeneration and oxidative damage to lipids, proteins and DNA. Mol Asp Med 32:305–315
46. Zhang H, Xiong Z, Wang J et al (2015) Glucagonlike peptide1 protects cardiomyocytes from advanced oxidation protein productinduced apoptosis via the PI3K/Akt/Bad signaling pathway. Mol Med Rep. doi:10.3892/mmr.2015.4724
47. Joshi S, Wei J, Bishopric NH (2015) A cardiac myocyte-restricted Lin28/let-7 regulatory axis promotes hypoxia-mediated apoptosis by inducing the AKT signaling suppressor PIK3IP1. Biochim Biophys Acta 1862:240–251
48. Zhang R, Li L, Yuan L, Zhao M (2015) Hypoxic preconditioning protects cardiomyocytes against hypoxia/reoxygenation-induced cell apoptosis via sphingosine kinase 2 and FAK/AKT pathway. Exp Mol Pathol 100:51–58
49. Okada M, Yamawaki H (2015) Levosimendan inhibits interleukin-1beta-induced apoptosis through activation of Akt and inhibition of inducible nitric oxide synthase in rat cardiac fibroblasts. Eur J Pharmacol 769:86–92
50. Cho S, Cho M, Kim J, Kaeberlein M, Lee SJ, Suh Y (2015) Syringaresinol protects against hypoxia/reoxygenation-induced cardiomyocytes injury and death by destabilization of HIF-1alpha in a FOXO3-dependent mechanism. Oncotarget 6:43–55